A Comparative XAS and X-ray Diffraction Study of New Binuclear Mn(III) Complexes with Catalase Activity. Indirect Effect of the Counteranion on Magnetic Properties

ARTICLE *in* INORGANIC CHEMISTRY · NOVEMBER 2004

Impact Factor: 4.76 · DOI: 10.1021/ic0348897 · Source: PubMed

5 AUTHORS, INCLUDING:

Gema Fernandez
TÜV Süd Group
6 PUBLICATIONS **111** CITATIONS
SEE PROFILE

Montserrat Corbella
University of Barcelona
72 PUBLICATIONS **1,544** CITATIONS
SEE PROFILE

Helen Stoeckli-Evans
Université de Neuchâtel
787 PUBLICATIONS **10,041** CITATIONS
SEE PROFILE

Isabel Castro
University of Valencia
72 PUBLICATIONS **2,368** CITATIONS
SEE PROFILE

Inorg. Chem. **2004**, *43*, 6684–6698

A Comparative XAS and X-ray Diffraction Study of New Binuclear Mn(III) Complexes with Catalase Activity. Indirect Effect of the Counteranion on Magnetic Properties

Gema Fernández,[†] Montserrat Corbella,*[,†] Montserrat Alfonso,[‡] Helen Stoeckli-Evans,[‡] and Isabel Castro[§]

Departament de Química Inorgànica, Facultat de Química, Universitat de Barcelona, Martí i Franquès 1-11, 08028-Barcelona, Spain, Institut de Chimie, Université de Neuchâtel, Avenue Bellevaux 51, CH-2007 Neuchâtel, Switzerland, and Departament de Química Inorgànica, Facultat de Química, Universitat de València, Dr. Moliner 50, 46100-Burjassot (València), Spain

Received July 28, 2003

Four new binuclear Mn(III) complexes with carboxylate bridges have been synthesized: $[\{Mn(nn)(H_2O)\}_2(\mu\text{-}ClCH_2COO)_2(\mu\text{-}O)](ClO_4)_2$ with nn = bpy (**1**) or phen (**2**) and $[\{Mn(bpy)(H_2O)\}_2(\mu\text{-}RCOO)_2(\mu\text{-}O)](NO_3)_2$ with RCOO = $ClCH_2COO$ (**3**) or CH_3COO (**4**). The characterization by X-ray diffraction (**1** and **3**) and X-ray absorption spectroscopy (XAS) (**1**–**4**) displays the relevance of this spectroscopy to the elucidation of the structural environment of the manganese ions in this kind of compound. Magnetic susceptibility data show an antiferromagnetic coupling for all the compounds: $J = -2.89$ cm^{-1} (for **1**), -8.16 cm^{-1} (for **2**), -0.68 cm^{-1} (for **3**), and -2.34 cm^{-1} (for **4**). Compounds **1** and **3** have the same cation complex $[\{Mn(bpy)(H_2O)\}_2(\mu\text{-}ClCH_2COO)_2(\mu\text{-}O)]^{2+}$, but, while **1** shows an antiferromagnetic coupling, for **3** the magnetic interaction between Mn(III) ions is very weak. The four compounds show catalase activity, and when the reaction stopped, Mn(II) compounds with different nuclearity could be obtained: binuclear $[\{Mn(phen)_2\}(\mu\text{-}ClCH_2COO)_2](ClO_4)_2$, trinuclear $[Mn_3(bpy)_2(\mu\text{-}ClCH_2COO)_6]$, or mononuclear complexes without carboxylate. Two Mn(II) compounds without carboxylate have been characterized by X-ray diffraction: $[Mn(NO_3)_2(bpy)_2][Mn(NO_3)(bpy)_2(H_2O)]NO_3$ (**5**) and $[Mn(bpy)_3](ClO_4)_2 \cdot 0.5\ C_6H_4\text{-}1,2\text{-}(COOEt)_2 \cdot 0.5H_2O$ (**8**).

Introduction

Interest in binuclear Mn(III) complexes with a carboxylate ligand is due to their presence in some metalloenzymes, such as the Mn-catalase. This enzyme, responsible for the disproportionation of H_2O_2 into H_2O and O_2, has been found in some bacteria, *Thermus thermophilus*, *Lactobacillus plantarum*, and *Thermoleophilum album*. The crystal structures of the enzymes from *Thermus thermophilus* and *Lactobacillus plantarum*[1,2] show that they have similar binuclear sites, with one carboxylate bridge and one or two bridging O-ligands from the solvent (oxo, hydroxo, or aqua). The reduced form has a $[Mn_2^{II}(\mu\text{-}OH)(\mu\text{-}H_2O)(\mu\text{-}GluCOO)]^{2+}$ core while the oxidized site presents two pH-dependent forms as $[Mn_2^{III}(\mu\text{-}O)(\mu\text{-}GluCOO)]^{3+}$ at low pH (6.5) or $[Mn_2^{III}(\mu\text{-}O)_2(\mu\text{-}GluCOO)]^{+}$ at high pH (9.5).[3] A possible mechanism for the process has been described, in which the H_2O_2 could be coordinated to one Mn(III) ion, in a monodentate fashion in the oxidized form, while it could bridge both Mn(II) ions in the reduced form.[2,4] But there are other Mn-enzymes, such as the water oxidase enzyme (WOE) in the photosynthetic center (PSII) of green plants whose structure and mechanism remain unclear. It is postulated as a tetra-

* To whom correspondence should be addressed. E-mail: montse.corbella@ub.edu.
[†] Universitat de Barcelona.
[‡] Université de Neuchâtel.
[§] Universitat de València.

(1) (a) Barynin, V. V.; Hempstead, P. D.; Vagin, A. A.; Antonyuk, S. V.; Melik-Adamyan, W. R.; Lamzin, V. S.; Harrison, P. M.; Artymiuk, P. J. *J. Inorg. Biochem.* **1997**, *67*, 196. (b) Antonyuk, S. V.; Melik-Adamyan, W. R.; Popov, A. N.; Lamzin, V. S.; Hempstead, P. D.; Harrison, P. M.; Artymiuk, P. J.; Barynin, V. V. *Crystallogr. Rep.* **2000**, *45*, 105.
(2) Barynin, V. V.; Whittaker, M. M.; Antonyuk, S. V.; Lamzin, V. S.; Harrison, P. M.; Artymiuk, P. J.; Whittaker, J. W. *Structure* **2001**, *9*, 725.
(3) Michaud-Soret, I.; Jacquamet, V.; Debaecker-Petit, N.; Le Pape, L.; Barynin, V. V.; Latour, J. M. *Inorg. Chem.* **1998**, *37*, 3874.
(4) Whittaker, M. M.; Barynin, V. V.; Antonyuk, S. V.; Whittaker, J. W. *Biochemistry* **1999**, *38*, 9126.

10.1021/ic0348897 CCC: $27.50
Published on Web 09/16/2004

nuclear site, and some authors suggest that this site is a dimer of dimers,[5] with oxo, or oxo and carboxylate, bridges, and only one of these dimers would be the catalytic center.[6,7] Therefore, the synthesis of new binuclear compounds of Mn(III), with carboxylate ligands, can contribute to a better knowledge of these biomolecules.

X-ray absorption spectroscopy (XAS) is a good method for studying the structure and oxidation state of manganese in water oxidase (WOE),[5,6,8] Mn-catalase,[9] or other enzymes. The structural and oxidation state changes in the S-states of the WOE could be clarified by comparison with model compounds. However, the characterization of binuclear Mn(III) complexes by XAS measurements is not usual. We found only one compound mentioned in the literature.[10]

On the other hand, although several binuclear Mn(III) complexes with a $[Mn_2(\mu\text{-}RCOO)_2(\mu\text{-}O)]^{2+}$ core have been described in the literature,[11−21] the structure and magnetic properties were only reported for some of them.[12−19] Also, in contrast with analogous compounds with Fe(III), the magnetic properties show a certain versatility: the magnetic coupling could be ferro- or antiferromagnetic.

The aim of this work was the synthesis of new binuclear Mn(III) complexes, with oxo and chloroacetate bridges, and terminal aromatic amine ligands, with a general formula $[\{Mn(nn)(H_2O)\}_2(\mu\text{-}ClCH_2COO)_2(\mu\text{-}O)](X)_2$. In a previous work,[22] we reported analogous compounds with chlorobenzoate bridges. In that case, we found that the magnetic properties of $[\{Mn(bpy)(H_2O)\}_2(\mu\text{-}2\text{-}ClC_6H_4COO)_2(\mu\text{-}O)](X)_2$ are different for different counteranions. If $X = NO_3$, the magnetic coupling was ferromagnetic, while for $X = ClO_4$ an antiferromagnetic interaction was found. In this work, we also synthesized the compounds with both anions, nitrate and perchlorate, with the intention of observing the effect on their magnetic properties. In this case, it has been possible to characterize, by X-ray diffraction, the two compounds obtained with the same cationic complex $[\{Mn(bpy)(H_2O)\}_2(\mu\text{-}ClCH_2COO)_2(\mu\text{-}O)]^{2+}$ and different anions. In order to make a further comparison with the acetate complex described in the literature,[12] $[\{Mn(bpy)(H_2O)\}_2(\mu\text{-}CH_3COO)_2(\mu\text{-}O)](PF_6)_2$, the analogous compound with nitrate as counteranion was prepared. Four new compounds are described in this paper: $[\{Mn(bpy)(H_2O)\}_2(\mu\text{-}ClCH_2COO)_2(\mu\text{-}O)](ClO_4)_2$ (**1**), $[\{Mn(phen)(H_2O)\}_2(\mu\text{-}ClCH_2COO)_2(\mu\text{-}O)](ClO_4)_2$ (**2**), $[\{Mn(bpy)(H_2O)\}_2(\mu\text{-}ClCH_2COO)_2(\mu\text{-}O)](NO_3)_2$ (**3**), and $[\{Mn(bpy)(H_2O)\}_2(\mu\text{-}CH_3COO)_2(\mu\text{-}O)](NO_3)_2$ (**4**). XAS measurements for all of them are reported; the comparison of both X-ray techniques (XAS and X-ray diffraction) for **1** and **3** allows us, on one hand, to confirm the validity of the XAS method in the structural determination of this kind of compounds, and on the other hand, it reports new data to compare with those of the Mn-enzymes.

We also report here on the H_2O_2 disproportionation reaction catalyzed by these Mn(III) binuclear complexes, the kind of Mn(II) compounds obtained when the reaction stopped, and the efficiency of the Mn(III) compounds as catalysts.

Experimental Section

Synthesis. All manipulations were performed under aerobic conditions. Organic reagents were used as received. Absolute ethanol QP, partially denatured, containing a 0.3% v/v of diethyl phthalate, was used. NBu_4MnO_4 was prepared as described in the literature.[23] Yield was calculated from total available Mn.

Caution! *Perchlorate salts of compounds containing organic ligands are potentially explosive. Only small quantities of these compounds should be prepared and handled behind suitable protective shields.*

$[\{Mn(nn)(H_2O)\}_2(\mu\text{-}ClCH_2COO)_2(\mu\text{-}O)](ClO_4)_2$, with nn = bpy (1) or phen (2). Both compounds were synthesized as follows: chloroacetic acid (0.15 g, 1.6 mmol) was added to a solution of $Mn(ClO_4)_2 \cdot 6H_2O$ (0.45 g, 1.28 mmol) in MeCN. Then, NBu_4MnO_4 (0.11 g, 0.32 mmol) dissolved in MeCN was added to the solution, which immediately turned dark brown. Finally, an MeCN solution of 2,2′-bipyridine for **1** (0.25 g, 1.6 mmol) or 1,10-phenanthroline for **2** (0.29 g, 1.6 mmol) was added, and the resulting solution (total volume 30 mL) was stirred for some minutes. Small dark crystals were obtained from the solutions when they were left undisturbed in the refrigerator for several days. Suitable X-ray diffraction crystals of **1** were obtained from a MeCN/CH_2Cl_2 (1:1) solution of the product layered with hexanes, at room temperature. Compound **1**: yield 0.31 g (ca. 56%). Anal. Calcd for $C_{24}H_{24}Cl_4Mn_2N_4O_{15}$ (860.15): C, 33.51; H, 2.81; N, 6.51. Found: C, 34.0; H, 2.8; N, 6.6%. IR (KBr, cm^{-1}): 1611 (vs), 1460 (m), 1394 (s), 1130 (vs), 1110 (vs), 1085 (vs), 1045 (m), 775 (s), 736 (m), 624 (m). Molar conductivity in MeCN, 10^{-3} M: 289 Ω^{-1} cm^2 mol^{-1}. Compound **2**: Yield: 0.37 g (ca. 63%). Anal. Calcd

(5) Yachandra, V. K.; Sauer, K.; Klein, M. P. *Chem. Rev.* **1996**, *96*, 2927.
(6) Dau, H.; Iuzzolino, L.; Dittmer, J. *Biochim. Biophys. Acta* **2001,** *1503*, 24.
(7) Hillier, W.; Wydrzynski, T. *Biochim. Biophys. Acta* **2001**, *1503*, 197.
(8) (a) Haumman, M.; Grabolle, M.; Neisius, T.; Dau, H. *FEBS Lett.* **2002**, *512*, 116. (b) Kuzek, D.; Pace, R. J. *Biochim. Biophys. Acta* **2001**, *1503*, 123.
(9) (a) Stemmler, T. L.; Sossong, T. M., Jr.; Goldstein, J. I.; Ash, D. E.; Elgren, T. E.; Kurtz Jr., D. M.; Penner-Hahn, J. E. *Biochemistry* **1997**, *36*, 9847. (b) Stemmler, T. L.; Sturgeon, B. E.; Randall, D. W.; Britt, R. D.; Penner-Hahn, J. E. *J. Am. Chem. Soc.* **1997**, *119*, 9215.
(10) Sauer, K.; Yachandra, V. K.; Britt, R. D.; Klein, M. P. *Manganese Redox Enzymes*; Pecoraro, V. L., Ed.; VCH: New York, 1992; Chapter 8, p 158.
(11) Dave, B. C.; Czernuszewickz, R. S. *Inorg. Chim. Acta* **1998**, *281*, 25.
(12) Ménage, S.; Girerd, J.-J.; Gleizes, A.. *J. Chem. Soc., Chem. Commun.* **1988**, 431.
(13) Corbella, M.; Costa, R.; Ribas, J.; Fries, P. H.; Latour, J. M.; Ohrstrom, L.; Solans, X.; Rodríguez, V. *Inorg. Chem.* **1996**, *35*, 1857.
(14) (a) Wieghardt, K.; Bossek, U.; Ventur, D.; Weiss, J. *J. Chem. Soc., Chem. Commun.* **1985**, 347. (b) Wieghardt, K.; Bossek, U.; Nuber, B.; Weiss, J.; Bonvoisin, J.; Corbella, M.; Vitols, S. E.; Girerd, J. J. *J. Am. Chem. Soc.* **1988**, *110*, 7398.
(15) Bolm, C.; Meyer, N.; Raabe, G.; Weyhermüller, T.; Bothe, E. *Chem. Commun.* **2000**, 2435.
(16) Vincent, J. B.; Folting, K.; Huffman, C. J.; Christou, G. *Biochem. Soc. Trans.* **1988**, *16*, 2.
(17) Vincent, J. B.; Tsai, H. L.; Blackman, A. G.; Wang, S.; Boyd, P. D.; Folting, K.; Huffman, J. C.; Lobkovsky, E. B.; Hendrickson, D. N.; Christou, G. *J. Am. Chem. Soc.* **1993**, *115*, 12353.
(18) Sheats, J. E.; Czernuszewicz, R. S.; Dismukes, G. C.; Rheingold, A. L.; Petrouleas, V.; Stubbe, J. A.; Armstrong, W. H.; Beer, R. H.; Lippard, S. J. *J. Am. Chem. Soc.* **1987**, *109*, 1435.
(19) Wu, F. J.; Kurtz, D. M., Jr.; Hagen, K. S.; Nyman, P. D.; Debrunner, P. G.; Vankai, V. A. *Inorg. Chem.* **1990**, *29*, 5174.
(20) Ruiz, R.; Sangregorio, C.; Caneschi, A.; Rossi, P.; Gaspar, A. B.; Real, J. A.; Muñoz, M. C. *Inorg. Chem. Commun.* **2000**, 361.
(21) Reddy, K. R.; Rajasekharan, M. V.; Sukumar, S. *Polyhedron* **1996**, *15*, 4161.
(22) Albela, B.; Corbella, M.; Ribas, J. *Polyhedron* **1996**, *15*, 91.
(23) Sala, T.; Sargent, M. V. *J. Chem. Soc., Chem. Commun.* **1978**, 253.

for $C_{28}H_{24}Cl_4Mn_2N_4O_{15}$ (908.2): C, 37.03; H, 2.63; N, 6.17. Found: C, 37.0; H, 2.6; N, 6.1%. IR (KBr, cm^{-1}): 1616 (vs), 1525 (s), 1428 (s), 1409 (s), 1395 (s), 1147 (s), 1116 (vs), 1088 (vs), 861 (m), 742 (m), 721 (s), 630 (m). Molar conductivity in MeCN, 10^{-3} M: 287 Ω^{-1} cm^2 mol^{-1}.

[{Mn(bpy)(H_2O)}$_2$(μ-RCOO)$_2$(μ-O)](NO_3)$_2$ with RCOO = $ClCH_2COO$ (3) or CH_3COO (4). A solution of chloroacetic acid (0.15 g, 1.6 mmol) in MeCN, for compound **3**, or glacial acetic acid (1 mL, 1.6 mmol), for compound **4**, was added to a solution of $Mn(NO_3)_2 \cdot 4H_2O$ (0.32 g, 1.28 mmol) in MeCN. Then, NBu_4MnO_4 (0.11 g, 0.32 mmol) dissolved in MeCN was added to the colorless solution, which became dark brown. Finally, a MeCN solution of 2,2′-bipyridine (0.25 g, 1.6 mmol) was added, and the resulting solution (90 mL) was filtered to eliminate any impurities. The filtrate was left undisturbed for several hours, and the small brown crystals formed were filtered off and dried in air. Recrystallization of compound **3** (0.35 g) in MeCN (75 mL) with two drops of HNO_3 70% gave some brown crystals suitable for X-ray diffraction. Compound **3**: yield 0.35 g (ca. 70%). Anal. Calcd for $C_{24}H_{24}Cl_2Mn_2N_6O_{13} \cdot 0.15\ H_2O$ (787.96): C, 36.58; H, 3.11; N, 10.67; Cl, 9.00. Found: C, 36.4; H, 3.1; N, 10.8; Cl, 8.8%. IR (KBr, cm^{-1}): 1602 (vs), 1449 (m), 1385 (vs), 1312 (m), 1261 (m), 773 (m), 728 (m). Molar conductivity in MeCN, 10^{-3} M: 116 Ω^{-1} cm^2 mol^{-1}. Compound **4**: yield 0.37 g (ca. 82%). Anal. Calcd for $C_{24}H_{26}Mn_2N_6O_{13}$ (716.37): C, 40.24; H, 3.66; N, 11.73. Found: C, 40.4; H, 3.6; N, 11.9%. IR (KBr, cm^{-1}): 1602 (m), 1585 (s), 1447 (m), 1384 (vs), 1309 (m), 1038 (m), 775 (m), 730 (m). Molar conductivity in MeCN, 10^{-3} M: 118 Ω^{-1} cm^2 mol^{-1}.

[Mn(NO_3)$_2$(bpy)$_2$][Mn(NO_3)(bpy)$_2$(H_2O)]NO_3 (5). 2,2′-Bipyridine (bpy) (0.62 g, 4.0 mmol) in 30 mL of MeCN was added to a solution of $Mn(NO_3)_2 \cdot 4H_2O$ (0.51 g, 2 mmol) in 20 mL of the same solvent. The solution turned yellow, and a pale yellow precipitate was formed, filtered off, washed in ether, and dried in air. From the mother liquor, or from a diluted solution of this compound in EtOH or MeCN, it was possible to obtain some crystals suitable for X-ray diffraction. Yield: 0.84 g (ca. 84%). Anal. Calcd for $C_{40}H_{34}\ Mn_2N_{12}O_{13}$ (1000.67): C, 48.01; H, 3.42; N, 16.80. Found: C, 48.2; H, 3.4; N, 16.5%. IR (KBr, cm^{-1}): 1769 (w), 1598 (s), 1578 (m), 1479 (m), 1440 (m), 1387 (vs), 1023 (s), 828 (m), 775 (s), 742 (m). Molar conductivity in MeCN, 10^{-3} M: 133 Ω^{-1} cm^2 mol^{-1}.

[Mn(nn)$_3$](ClO_4)$_2$ with nn= bpy (6) or phen (7). Bidentate amine (4 mmol; 0.62 g of 2,2′-bipyridine for compound **6**, 0.72 g of 1,10-phenantroline for compound **7**) was added to an ethanolic solution of 0.72 g (2 mmol) of $Mn(ClO_4)_2 \cdot 6\ H_2O$ (20 mL of EtOH). The mixture turned yellow, and a yellow precipitate of [Mn(nn)$_3$](ClO_4)$_2$ was formed very quickly. Yield for **6**: 1.37 g (ca. 94%). Anal. Calcd for $C_{30}H_{24}Cl_2MnN_6O_8 \cdot 0.5\ H_2O$ (731.4): C, 49.25; H, 3.42; N, 11.49. Found: C, 48.1; H, 3.4; N, 11.5%. IR (KBr, cm^{-1}): 1591 (m), 1479 (m), 1460 (m), 1440 (s), 1420 (s), 1150 (vs), 1117 (vs), 1085 (vs), 1019 (m), 782 (s), 762 (m), 742 (m), 624 (s). Molar conductivity in MeCN, 10^{-3} M: 299 Ω^{-1} cm^2 mol^{-1}. Yield for **7**: 1.50 g (ca. 89%). Anal. Calcd for $C_{36}H_{24}Cl_2MnN_6O_8 \cdot 3H_2O$ (848.5): C, 50.94; H, 3.54; N, 9.90. Found: C, 51.1; H, 3.5; N, 9.9%. IR (KBr, cm^{-1}): 1627 (w), 1598 (w), 1525 (m), 1435 (s), 1150 (vs),1117 (vs), 1091 (vs), 841 (s), 729 (s), 644 (s), 624 (s).

[Mn(bpy)$_3$](ClO_4)$_2 \cdot 0.5C_6H_4$-1,2-(COOEt)$_2 \cdot 0.5H_2O$ (8). When the mother liquor of compound **6** was left undisturbed in open air, orange needles of compound **8** were obtained. The same compound was also found by recrystallization of [Mn(bpy)$_3$](ClO_4)$_2$ (**6**) in an EtOH−H_2O mixture. X-ray diffraction showed that the crystalline product was [Mn(bpy)$_3$](ClO_4)$_2 \cdot 0.5C_6H_4$-1,2-(COOEt)$_2 \cdot 0.5H_2O$ (**8**). Anal. Calcd for $C_{30}H_{24}Cl_2MnN_6O_8 \cdot 0.5C_{12}H_{14}O_4 \cdot 0.5H_2O$: C, 51.31; H, 3.80; N, 9.98. Found: C, 51.2; H, 3.8; N, 9.9%. IR (KBr, cm^{-1}): 1723 (s), 1591 (s), 1479 (m), 1447 (m), 1420 (m), 1289 (s), 1150 (vs), 1117 (vs), 1091 (vs), 1019 (m), 782 (s), 742 (m), 624 (s).

[{Mn(bpy)(H_2O)}$_2$(μ-CH_3COO)$_2$(μ-O)](PF_6)$_2$ (9)[12] and [{Mn(OH)(bpy)}(μ-PhCOO)$_2$(μ-O){Mn(NO_3)(bpy)}]$\cdot H_2O$ (10)[13] were prepared as described in the literature. Anal. Calcd for $C_{24}H_{30}F_{12}Mn_2N_4O_9P_2$ (**9**): C, 31.39; N, 6.1; H, 3.29. Found: C, 31.3; N, 6.0; H, 3.3. Anal. Calcd for $C_{34}H_{29}Mn_2N_5O_{10}$ (**10**): C, 52.52; N, 9.01; H, 3.76. Found: C, 52.4; N, 9.1; H, 3.6%.

Catalase Activity. An MeCN solution (20 mL) of binuclear Mn(III) complexes (**1**−**4**) (1 mM) was treated with 1 mL of H_2O_2 (30 wt %). The brown color of the solution disappeared immediately, and a large emission of O_2 was observed. The intensity of the evolved oxygen decreased after few minutes, and 15 min after the beginning of the reaction, this evolution turned monotonic, and a little brown and very fine solid was observed. After 3 h, the reaction came to an end. The brown solid was filtered, and the yellow solution was kept undisturbed at room temperature. After some days, different Mn(II) compounds were obtained in each case.

For the nitrate complexes, **3** and **4**, we also tested the effect of the addition of $NaClO_4$ to the yellow solution obtained at the end of the reaction. Then, to these solutions 0.025 g of $NaClO_4 \cdot H_2O$ (0.18 mmol) was added with stirring, and the resultant mixture was kept undisturbed for some days until precipitation of the Mn(II) compound.

The extent of the reaction was followed by measurement of the oxygen volume evolved from the reaction of 5 mL of a 0.8 mM acetonitrile solution of the binuclear Mn(III) complex, at room temperature, with 0.3 mL of H_2O_2 (8.8 M). Aliquots were taken after 1 min and transferred into an EPR tube (and frozen with liquid N_2) or injected into an ES-MS spectrometer. Conductivity measurements along the reaction were also carried out.

Physical Measurements. Analyses of C, H, N, and Cl were carried out by the "Serveis Científico-Tècnics" of the Universitat de Barcelona. Infrared spectra (4000−400 cm^{-1}) were recorded from KBr pellets in a Nicolet Impact 400 FT-IR spectrometer. Conductivity measurements were carried out with a CRISON instrument Micro CN 2200, at 20 °C. Electrospray mass spectra (ES-MS) were recorded on a Fisons VG Quattro spectrometer, by the "Servei de Masses" of the Universitat de Barcelona. Magnetic susceptibility measurements were performed on a MANICS-DSM8 susceptometer equipped with an Oxford Instruments liquid helium cryostat, working down to 4.2 K, at the "Servei de Magnetoquímica" (Universitat de Barcelona). Pascal's constants were used to estimate the diamagnetic corrections for each complex. The fits were performed by minimizing the function $R = \sum(\chi_{Mexp} - \chi_{Mcalc})^2/\sum(\chi_{Mexp})^2$ (for compounds **1**, **2**, and **4**) or $R = \sum(\chi_M \cdot T_{exp} - \chi_M \cdot T_{calc})^2/\sum(\chi_M \cdot T_{exp})^2$ (for **3**). EPR spectra were recorded at X-band (9.4 GHz) frequencies with a Bruker ESP-300E spectrometer, at the "Servei de Magnetoquímica" of the Universitat de Barcelona.

X-ray Diffraction Data Collection and Refinement. A brown crystal of [{Mn(bpy)(H_2O)}$_2$(μ-$ClCH_2COO$)$_2$(μ-O)] (ClO_4)$_2 \cdot 1.9H_2O \cdot 2CH_3CN$ (**1**) (0.60 × 0.25 × 0.12 mm^3), a brown plate crystal of [{Mn(bpy)(H_2O)}$_2$(μ-$ClCH_2COO$)$_2$(μ-O)](NO_3)$_2 \cdot 0.15H_2O$ (**3**) (0.50 × 0.20 × 0.10 mm^3), a yellow needlelike crystal of [Mn(NO_3)$_2$(bpy)$_2$][Mn(NO_3)(bpy)$_2$(H_2O)]NO_3 (**5**) (0.60 × 0.23 × 0.19 mm^3), and a yellow block crystal of [Mn(bpy)$_3$](ClO_4)$_2 \cdot 0.5$[C_6H_4-1,2-(COOEt)$_2$]$\cdot 0.5H_2O$ (**8**) (0.35 × 0.35 × 0.17 mm^3) were chosen for X-ray diffraction experiments. The unit-cell and intensity data were measured with a Stoe Image Plate Diffraction system (compounds **1**, **3**, and **8**) and a Stoe-Siemens AED2 four-circle diffractometer (compound **5**), using Mo Kα graphite monochromated radiation. The structures were solved by direct methods using

Table 1. X-ray Crystallographic Data for the Mn(III) Compounds $[\{Mn(bpy)(H_2O)\}_2(\mu\text{-}ClCH_2COO)_2(\mu\text{-}O)](ClO_4)_2\cdot 1.9H_2O\cdot 2CH_3CN$ (**1**) and $[\{Mn(bpy)(H_2O)\}_2(\mu\text{-}ClCH_2COO)_2(\mu\text{-}O)](NO_3)_2\cdot 0.15H_2O$ (**3**), and for the Mn(II) Compounds $[Mn(NO_3)_2(bpy)_2][Mn(NO_3)(bpy)_2(H_2O)]NO_3$ (**5**) and $[Mn(bpy)_3](ClO_4)_2\cdot 0.5[C_6H_4\text{-}1,2\text{-}(COOEt)_2]\cdot 0.5H_2O$ (**8**)

	1	**3**	**5**	**8**
formula	$C_{28}H_{33.8}Cl_4Mn_2N_6O_{16.9}$	$C_{24}H_{24.3}Cl_2Mn_2N_6O_{13.15}$	$C_{40}H_{34}Mn_2N_{12}O_{13}$	$C_{36}H_{32}N_6Cl_2MnO_{10.5}$
fw	976.49	787.97	1000.67	842.52
space group	$P\bar{1}$	$P\bar{1}$	*Pbca*	$C222_1$
a, Å	10.779(2)	9.3310(7)	14.412(12)	24.775(2)
b, Å	12.499(2)	10.1002(8)	17.208(18)	13.8968(9)
c, Å	16.749(3)	17.9091(14)	34.69(2)	22.0113(15)
α, deg	82.28(3)	91.822(9)	90	90
β, deg	78.40(3)	91.083(9)	90	90
γ, deg	86.32(3)	117.395(8)	90	90
V, Å^3	2188.8(7)	1496.7(2)	8603(13)	7578.3(9)
Z	2	2	8	8
T, K	223(2)	153(2)	293(2)	223(2)
λ(Mo Kα), Å	0.71069	0.71073	0.71073	0.71073
ρ_{calc}, g/cm^3	1.482	1.748	1.545	1.477
R1[a] [$I > 2\sigma(I)$]	0.0638	0.0281	0.0877	0.0357
wR2[b] [$I > 2\sigma(I)$]	0.1532	0.0654	0.1931	0.0633
R1[a] [all data]	0.1104	0.0386	0.1575	0.0657
wR2[b] [all data]	0.1799	0.0689	0.2501	0.0704

[a] $R1 = \sum||F_o| - |F_c||/\sum|F_o|$. [b] $wR2 = \{\sum[w(F_o^2 - F_c^2)^2]/\sum[w(F_o^2)^2]\}^{1/2}$.

the program SHELXS-93[24] and refined by full-matrix least-squares on F^2 with SHELXL-97.[25] For **3**, the H-atoms were located using Fourier difference maps and refined isotropically, while for **1**, **5**, and **8** they were included in calculated positions and treated as riding atoms using the SHELXL default parameters. The non-H atoms were refined isotropically, using weighted full-matrix least-squares on F^2. Crystal data collection and refinement parameters are given in Table 1. Further details, concerning disorder (generally present in the anions), for example, are given in the crystallographic CIF files, which are available as Supporting Information.

X-ray Absorption Data Collection and Analysis. X-ray absorption spectra, both XANES (X-ray absorption near edge structure) and EXAFS (extended X-ray absorption fine structure) spectra of well-pounded microcrystalline powders were collected on a D42 beamline at LURE (Laboratoire d'Utilization du Rayonnement Electromagnetique, Paris-Sud University, France) with the storage ring operating at an energy of 1.85 GeV and a mean intensity of 300−200 mA. The measurements were taken at the manganese K-edge in the transmission mode on the XAS 13 spectrometer equipped with a two-crystal monochromator for energy selection (Si 311 and Si 111 for XANES and EXAFS, respectively); the entrance slit was 0.5 mm for both types of spectra. The monochromator was slightly detuned to ensure harmonics rejection. Reduced-pressure, air-filled ionization chambers were used to measure the flux intensity before and after the sample. XANES spectra were recorded at room temperature and EXAFS spectra at 10 K in a helium cryostat designed for X-ray absorption spectroscopy. Samples were of a homogeneous thickness and calculated weight to avoid saturation effects. The absorption jump at the edge was typically 1 and the total absorption above the edge less than 1.5.

XANES spectra were recorded over 150 eV step by step, every 0.3 eV with a 1 s accumulation time per point. The spectrum of a 5 μm thick manganese foil was recorded just after or before an unknown XANES spectrum to check the energy calibration, thus ensuring an energy accuracy of 0.3 eV. EXAFS spectra were recorded in the same way over 1200 eV, with 3 eV steps and 2 s accumulation time per point. For energy reference, a metal foil was measured together with each sample. The energy threshold $E_{0,ref}$ of the metal foil was determined from the first inflection point in the spectrum, and raw data were linearly calibrated against the difference between the obtained $E_{0,exp}$ and the tabulated absorption edge energy (Mn K edge $E_{0,ref} = 6539$ eV).[26] Each spectrum is the average of several independent recordings added after individual inspection (two for XANES and four for EXAFS). XANES spectra were processed by subtracting a linear background computed by least-squares fitting from the preedge experimental points and normalized at the middle of the first EXAFS oscillation using the "GALAAD"[27] program. Edge energies for all XANES spectra were taken as the first inflection point on the rising edge, determined from the second derivate zero crossing.[5] The 1s → 3d areas were determined by first fitting an arctangent background to the normalized data below and above the 1s → 3d transition. The normalized area of the pre-edge peak after background subtraction was obtained by numerical integration over the range 6534−6544 eV and is expressed in units of 10^{-2} eV.[28] Mn(III) is highly susceptible to photoreduction when exposed to intense X-rays, mainly at elevated (i.e., room) temperatures, and the XANES spectra were collected at room temperature. In order to discard the presence of some reduction, the XANES spectra, at room temperature, were compared with the corresponding part of the EXAFS spectra at 10 K (Figure S1, Supporting Information). The spectra are coincident for all compounds within the resolution limits.

The standard EXAFS data analysis was performed with the *EXAFS pour le MAC*[29] program following a well-known procedure described elsewhere.[30,31] This analysis includes linear pre-edge background removal, a cubic 4 region spline atomic absorption energy-dependent procedure, Lengeler−Eisenberger EXAFS spectra normalization, and reduction from the absorption data $\mu(E)$ to the EXAFS spectrum $\chi(k)$ with

$$k = \sqrt{\frac{2m}{\hbar^2}(E - E_0)}$$

where E_0 is the energy threshold, taken at the absorption maximum (6558.02 eV). Radial distribution functions $F(R)$ were calculated by Fourier transforms of $k^3w(k)\chi(k)$ in the 2−16 Å^{-1} k range; $w(k)$ is a Kaiser−Bessel apodization window with a smoothness coefficient of $\tau = 3$. After Fourier filtering, the first Mn shell was fitted, in the 2.5−15.5 Å^{-1} k range (resolution $\pi/2\partial k = 0.12$ Å). The analysis has been done considering 4 layers. Amplitude and phase functions for different elements of backscatters used to simulate experimental data were calculated using the FEFF program (version 6.01)[32] over the model compound $[\{Mn(bpy)(H_2O)\}_2(\mu\text{-}CH_3COO)_2(\mu\text{-}O)](PF_6)_2$ (**9**) synthesized as described in the literature.[12]

(24) Sheldrick, G. M. *Acta Crystallogr.* **1990**, *A46*, 467.
(25) Sheldrick, G. M. *SHELXL-97, Program for crystal structure refinement*; University of Göttingen: Göttingen, Germany, 2001.
(26) Bearden, J. A.; Burr, A. F. *Rev. Mod. Phys.* **1967**, *39*, 125.
(27) Noinville, V.; Michalowicz, A. *GALAAD in Logiciels pour la Chimie*; Société Française de Chimie: Paris, 1991; pp 116−117.
(28) Roe, A. L.; Schneider, D. J.; Mayer, R. J.; Pyrz, J. W.; Widom, J.; Que, L. J. *J. Am. Chem. Soc.* **1984**, *106*, 1676.
(29) Michalowicz, A. EXAFS pour le MAC: a new version of an EXAFS data analysis code for the Macintosh. *J. Phys. IV* **1997**, *7*, 235.
(30) Teo, B. K. *EXAFS: basic principles and data analysis*; Springer-Verlag: Berlin, 1986; Vol. 9.
(31) Real, J. A.; Castro, I.; Bousseksou, A.; Verdaguer, M.; Burriel, R.; Castro, M.; Linares, J.; Varret, F. *Inorg. Chem.* **1997**, *36*, 455.
(32) Rehr, J. J.; Zabinsky, S. I.; Albers, R. C. *Phys. Rev. Lett.* **1992**, *69*, 3397.

Results and Discussion

Synthesis. The synthetic method used to obtain the binuclear Mn(III) complexes is a comproportionation reaction between Mn(II) and MnO_4^- in the presence of carboxylic acid and bidentate amine. The stoichiometry of this reaction is

$$1.6MnX_2 + 2RCOOH + 0.4NBu_4MnO_4 + 2nn \rightarrow [\{Mn(nn)(H_2O)\}_2(\mu\text{-}RCOO)_2(\mu\text{-}O)]X_2$$

where X = NO_3, ClO_4; nn = bpy, phen; and RCOO = $ClCH_2COO$, CH_3COO.

Attempts to obtain the binuclear Mn(III) complex with $ClCH_2COO^-$, phenanthroline, and nitrate anion were unsuccessful. On the other hand, with acetate bridges, only the complex with nitrate anion and bipyridine ligand was synthesized. In this kind of reaction, after removing all the Mn(III) complex, the residual pale brown solution gave a Mn(II) complex, without carboxylate ligand, **5**, **6**, or **7**. The same compounds were obtained in some cases by reaction of the binuclear Mn(III) complexes with H_2O_2, and it is also possible to obtain them by direct reaction between the proper Mn(II) salt and the bidentate amine. An important structural difference was observed between Mn(II) complexes **5** and **8**. The former shows two bpy ligands, and two nitrate anions (or one nitrate and one water molecule) coordinated to the Mn(II), while in the perchlorate complex there are three bpy ligands coordinated to the manganese ion. In the IR spectrum of compound **5**, a weak and very narrow band assigned to the nitrate ligand ($\nu_1 + \nu_3$) was observed at ~1770 cm^{-1}.[33] On the other hand, when the perchlorate compound $[Mn(bpy)_3](ClO_4)_2$, **6**,[34] was crystallized from an ethanolic solution, two new strong bands appeared at 1723 and 1290 cm^{-1} in the IR spectrum. The crystal structure of the new compound (**8**) showed the incorporation of C_6H_4-1,2-$(COOEt)_2$ into the crystal lattice. This additive is present in a small quantity in the used ethanol. The new bands observed in the IR spectrum could be assigned to the C═O group of this molecule.[33]

The molar conductivity values for the solutions of binuclear Mn(III) complexes with perchlorate anions (**1** and **2**) agree with what is expected for 1:2 electrolytes in acetonitrile (220−300 Ω^{-1} cm^2 mol^{-1}).[35] On the other hand, the values of molar conductivity for the complexes with nitrate anions (**3** and **4**) were close to the expected values for 1:1 electrolytes (120−160 Ω^{-1} cm^3 mol^{-1}).[35] After these results, we can suppose that in a MeCN solution the nitrate anion shows a certain tendency to coordinate to the manganese ion.

Description of the Structures. $[\{Mn(bpy)(H_2O)\}_2(\mu\text{-}ClCH_2COO)_2(\mu\text{-}O)](ClO_4)_2\cdot 1.9H_2O\cdot CH_3CN$ (1) and $[\{Mn(bpy)(H_2O)\}_2(\mu\text{-}ClCH_2COO)_2(\mu\text{-}O)](NO_3)_2\cdot 0.15H_2O$ (3). Both complexes have the same binuclear Mn(III) cationic complex: $[\{Mn(bpy)(H_2O)\}_2(\mu\text{-}ClCH_2COO)_2(\mu\text{-}O)]^{2+}$. The ORTEP drawings are shown in Figure 1. Selected interatomic bond distances and angles are listed in Table 2.

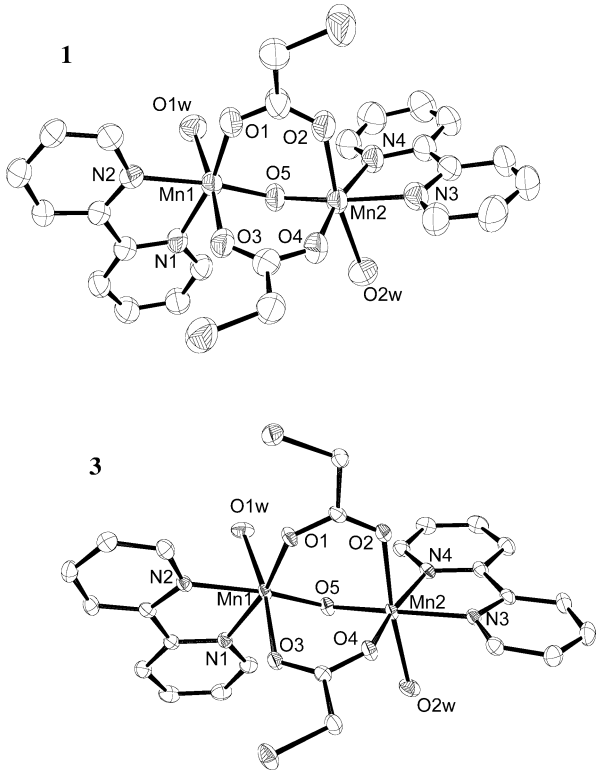

Figure 1. Crystal structures of the cation complex $[\{Mn(bpy)(H_2O)\}_2(\mu\text{-}ClCH_2COO)_2(\mu\text{-}O)]^{2+}$ in **1** (top) and **3** (bottom), showing 50% probability thermal ellipsoids. Hydrogen atoms are omitted for clarity.

Table 2. Selected Bond Distances (Å) and Angles (deg) for Compounds **1** and **3**

	1	**3**
Mn(1)−O(5)	1.782(4)	1.787(2)
Mn(1)−O(1)	1.948(4)	1.9574(2)
Mn(1)−N(2)	2.061(4)	2.070(2)
Mn(1)−N(1)	2.068(5)	2.073(2)
Mn(1)−O(3)	2.224(4)	2.270(2)
Mn(1)−O(w1)	2.240(4)	2.186(2)
Mn(2)−O(5)	1.792(4)	1.789(1)
Mn(2)−O(4)	1.945(4)	1.959(1)
Mn(2)−N(4)	2.056(5)	2.059(2)
Mn(2)−N(3)	2.058(5)	2.064(2)
Mn(2)−O(2)	2.162(4)	2.218(2)
Mn(2)−O(w2)	2.262(4)	2.213(2)
Mn(1)−Mn(2)	3.1657(11)	3.1662(5)
Mn(2)−O(5)−Mn(1)	124.7(2)	124.6(1)
O(5)−Mn(1)−N(2)	170.4(2)	170.4(1)
O(1)−Mn(1)−N(1)	168.6(2)	168.1(1)
O(3)−Mn(1)−O(w1)	174.1(2)	171.0(1)
O(5)−Mn(2)−N(3)	170.3(2)	170.3(1)
O(4)−Mn(2)−N(4)	168.2(2)	168.4(1)
O(2)−Mn(2)−O(w2)	171.5(2)	172.4(1)

The cationic complex shows two chloroacetate and one oxo bridges. Compound **1** shows a disposition of the carboxylate bridges with the Cl atoms on opposite sides, while for complex **2** both Cl atoms are on the same side. A chelating 2,2′-bipyridine (bpy) acting as terminal ligand and one water molecule complete the octahedral coordination of each manganese atom.

(33) Nakamoto, K. *Infrared and Raman Spectra of Inorganic and Coordination Compounds*, 5th ed.; John Wiley & Sons: New York, 1997.
(34) Yu, X.-L.; Tong, Y.-X.; Chen, X.-M.; Mak, T. C. W. *J. Chem. Crystallogr.* **1997**, *27*, 441.
(35) Geary, W. J. *Coord. Chem. Rev.* **1971**, *7*, 81.

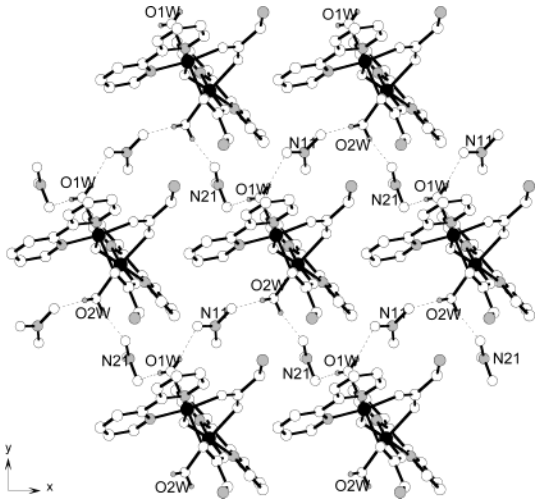

Figure 2. Hydrogen bonds through the nitrate anion for compound **3**.

Most structural parameters are very similar for both compounds: d(Mn···Mn) ≈ 3.166 Å, d(Mn−O_{bridge}) ≈ 1.787 Å, α(Mn−O−Mn) = 124.6°, d(Mn−N) ≈ 2.06 Å, and, also for the carboxylate ligand trans to bpy ligand, d(Mn−O_{transN}) ≈1.95 Å. In both complexes, the manganese ions show an elongated octahedral environment in the water-carboxylate direction. Some small differences between the two complexes are observed. In complex **1**, the distance d(Mn−O_w) is greater than d(Mn−O_{transW}) (av 2.25 compared to 2.19 Å), while for complex **3** the distance d(Mn−O_{transW}) is greater than d(Mn−O_w) (av 2.24 compared to 2.20 Å). The torsion angle O(1w)−Mn(1)−Mn(2)−O(2w) is also different for both compounds: −96.9(2)° for compound **1** and −109.7(1)° for compound **3**. The structural differences related to the aqua ligands could be due to hydrogen bonds, which are present in compound **3**. Each nitrate anion bonds two binuclear complexes, through Mn(1)−OH_2···NO_3···H_2O−Mn(2), and each H_2O ligand bonds to two nitrate anions; the result is a wavy sheet in the *xy* plane (Figure 2). Because of this hydrogen bond network, four binuclear complexes and four nitrate anions are arranged to form rings, in each sheet.

A compound similar to **1** has been described in the literature: [{Mn(bpy)(MeOH)}(μ-$ClCH_2COO$)$_2$(μ-O){Mn(bpy)(H_2O)}](ClO_4)$_2$.[11] There, the disposition of the Cl atoms is the same as that found in compound **1**. An important difference between both compounds is the coordination of a molecule of MeOH to one of the manganese ions. The structural parameters are also quite different: d(Mn···Mn) = 3.160 Å, d(Mn−O_{bridge}) ≈ 1.793 Å, α(Mn−O−Mn) = 123.5°, d(Mn−N) ≈ 2.060 Å, and, also for the carboxylate ligand trans to bpy ligand, d(Mn−O_{transN}) ≈ 1.94 Å. Similarly to compound **1**, distance d(Mn−$O_{trans\ to\ L}$) < d(Mn−O_L), where L = MeOH or H_2O [d(Mn−$O_{trans\ to\ MeOH}$) = 2.178 Å, d(Mn−O_{MeOH}) = 2.287 Å, d(Mn−$O_{trans\ to\ W}$) = 2.206 Å, d(Mn−O_w) = 2.214 Å]. However, distance d(Mn−MeOH) > d(Mn−OH_2); therefore, the elongation around each manganese ion is slightly different.

Structure of [Mn(NO$_3$)$_2$(bpy)$_2$][Mn(NO$_3$)(bpy)$_2$(H_2O)]NO$_3$ (5). The unit cell contains two different Mn(II) mononuclear complexes, one neutral and the other cationic, together with a nitrate counterion. The three entities are represented in Figure 3.

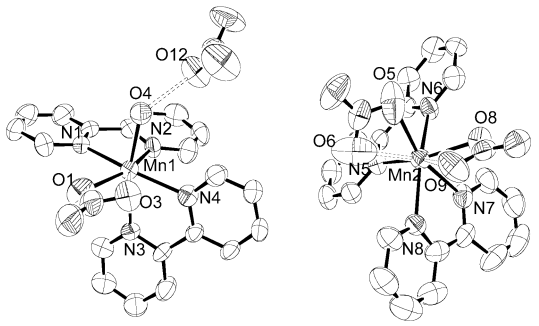

Figure 3. ORTEP view of the three groups present in **5** (ellipsoids at 50% probability, hydrogen atoms omitted for clarity).

Table 3. Selected Bond Distances (Å) and Angles (deg) for Compound **5**

Mn(1)−O(4)	2.156(8)	Mn(2)−N(5)	2.250(10)
Mn(1)−O(1)	2.251(10)	Mn(2)−O(8)	2.255(8)
Mn(1)−N(3)	2.266(9)	Mn(2)−N(8)	2.254(9)
Mn(1)−N(4)	2.258(9)	Mn(2)−N(6)	2.287(10)
Mn(1)−N(1)	2.283(10)	Mn(2)−O(5)	2.336(14)
Mn(1)−N(2)	2.334(10)	Mn(2)−N(7)	2.365(10)
Mn(1)−O(3)	2.860(12)	Mn(2)−O(6)	2.565(16)
O(4)···O(12)	2.611(13)	Mn(2)−O(9)	2.872(10)
O(4)−Mn(1)−N(3)	167.3(3)	N(5)−Mn(2)−O(8)	154.7(3)
N(4)−Mn(1)−N(1)	159.4(4)	O(8)−Mn(2)−N(8)	102.3(3)
O(1)−Mn(1)−N(2)	153.7(4)	N(8)−Mn(2)−N(6)	155.0(4)
O(1)−Mn(1)−O(3)	47.1(3)	N(8)−Mn(2)−O(5)	125.9(5)
O(6)−Mn(2)−O(5)	48.9(4)	O(5)−Mn(2)−N(7)	160.3(4)
O(9)−Mn(2)−O(8)	47.7(3)		

Both complexes show a very distorted octahedral environment for the Mn(II) ion. Each manganese ion has two 2,2′-bipyridine ligands (bpy) in a cis disposition. The neutral complex (Figure 3, right side) has two nitrate ligands, while the cationic complex (Figure 3, left side) has one nitrate ligand and one water molecule. The most important distances and angles are given in Table 3. The disposition of the nitrate ligand, with another oxygen atom near the manganese center (O(3) for Mn(1), and O(6) and O(9) for Mn(2)), provokes a significant distortion of the octahedral geometry.

Two sets of Mn−N_{bpy} distances were observed: av 2.27 Å for N_{bpy} trans to N_{bpy} or av 2.34 Å for N_{bpy} trans to $O_{nitrate}$. This difference was also observed for N_{bpy} trans to $O_{carboxylate}$.[36−39]

The nitrate ligand in the cationic complex and one of the nitrate ligands in the neutral complex show a similar Mn−$O_{nitrate}$ distance (av. 2.25 Å). This distance is greater for the second nitrate of the neutral unit (2.34 Å). The Mn−O_w distance (2.156 Å) in the cationic complex is shorter than the Mn(III)−OH_2 distance found for compounds **1** and **3**, but it is similar to the values found in other Mn(II) complexes described in the literature.[40,41] A hydrogen bonding interac-

(36) Albela, B.; Corbella, M.; Ribas, J.; Castro, I.; Sletten, J.; Stoeckli-Evans, H. *Inorg. Chem.* **1998**, *37*, 788.
(37) Lubben, M.; Meetsma, A.; Feringa, B. L. *Inorg. Chim. Acta* **1995**, *230*, 169.
(38) Lumme, P. O.; Lindell, E. *Acta Crystallogr.* **1988**, *44*, 463.
(39) Fernández, G.; Corbella, M.; Mahía, J.; Maestro, M. *Eur. J. Inorg. Chem.* **2002**, 2502.
(40) Kitajima, N.; Sihgh, U. P.; Amagai, H.; Osawa, M.; Moro-oka, Y. *J. Am. Chem. Soc.* **1991**, *113*, 7757.

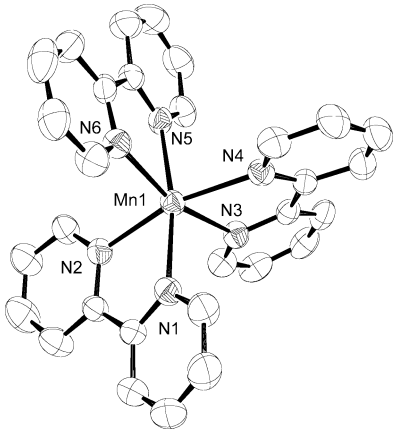

Figure 4. ORTEP view of $[Mn(bpy)_3]^{2+}$ cation in **8** (ellipsoids at 50% probability, hydrogen atoms omitted for clarity).

Table 4. Selected Bond Lengths (Å) and Angles (deg) for Compound $[Mn(bpy)_3](ClO_4)_2 \cdot 0.5(C_6H_4\text{-}1,2\text{-}(COOEt)_2) \cdot 0.5H_2O$ (**8**)

Mn(1)−N(6)	2.191(2)
Mn(1)−N(2)	2.216(3)
Mn(1)−N(4)	2.221(3)
Mn(1)−N(1)	2.265(3)
Mn(1)−N(3)	2.252(2)
Mn(1)−N(5)	2.273(2)
N(2)−Mn(1)−N(4)	165.36(9)
N(6)−Mn(1)−N(3)	163.13(9)
N(1)−Mn(1)−N(5)	170.13(9)

tion between the coordinated water molecule and the nitrate anion was observed [$d(O_w-O_{nitrate}) = 2.613$ Å].

Both complexes show a distorted octahedral geometry. In the case of the Mn(1) ion, the coordination octahedron is compressed in the direction of the water axis [O(4)−Mn(1)−N(3)], while for the Mn(2) ion the coordination octahedron is elongated on the more labile nitrate axis [O(5)−Mn(2)−N(7)].

Structure of $[Mn(bpy)_3](ClO_4)_2 \cdot 0.5(C_6H_4\text{-}1,2\text{-}(COOEt)_2) \cdot 0.5H_2O$ (8). The bond lengths and angles for compound **8** are listed in Table 4. The manganese ion shows an octahedral environment, created by three bipyridine ligands (Figure 4).

The Mn−N distances range from 2.19 to 2.27 Å, and a slight elongation of the octahedral environment was observed in the N(1)−Mn(1)−N(7) direction. The N−Mn−N angles for the nitrogen atoms of the same bpy ligand are av 73.4°, but for the nitrogen atoms of different bpy ligands, this value is in the range 91.02−98.30°.

XANES and EXAFS Spectra. Attempts to obtain X-ray-quality crystals for compounds **2** and **4** failed. Compounds **1** and **3** show some differences in their structural parameters, despite having the same cation complexes, and differing only in the counteranion. Therefore, we decided to study the XANES and EXAFS spectra of the four compounds. (Table 5 lists the different compounds mentioned in this paper.) Compound **2** has the same carboxylate as **1** and **3**, but a different amine (phen instead of bpy), while compound **4** has the same amine as **1** and **3** (bpy), but a different carboxylate (acetate instead of chloroacetate). A compound

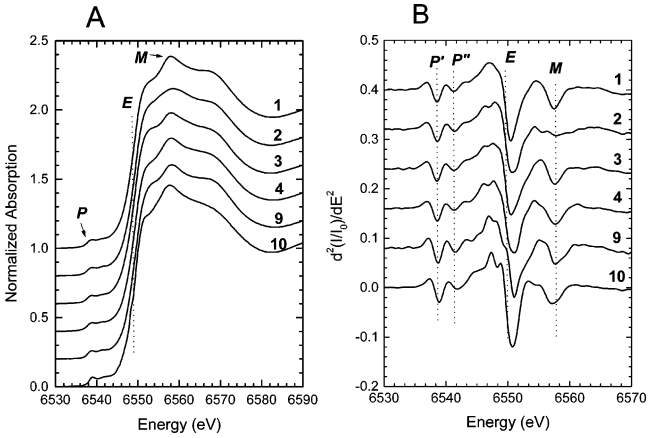

Figure 5. (A) Normalized XANES spectra at the Mn K-edge for compounds **1**−**4**, **9**, and **10**. (B) Their corresponding second derivatives. The cation complex is $[\{Mn(bpy)(H_2O)\}_2(\mu\text{-}ClCH_2COO)_2(\mu\text{-}O)]^{2+}$ for compounds **1** and **3**, $[\{Mn(phen)(H_2O)\}_2(\mu\text{-}ClCH_2COO)_2(\mu\text{-}O)]^{2+}$ for **2**, $[\{Mn(bpy)(H_2O)\}_2(\mu\text{-}CH_3COO)_2(\mu\text{-}O)]^{2+}$ for **4** and **9**, and $[\{Mn(OH)(bpy)\}(\mu\text{-}PhCOO)_2(\mu\text{-}O)\{Mn(NO_3)(bpy)\}]$ for **10**.

Table 5. Compounds Referred to throughout This Paper

		ref
	Binuclear Mn(III) Compounds	
1	$[\{Mn(bpy)(H_2O)\}_2(\mu\text{-}ClCH_2COO)_2(\mu\text{-}O)](ClO_4)_2$	*a*
2	$[\{Mn(phen)(H_2O)\}_2(\mu\text{-}ClCH_2COO)_2(\mu\text{-}O)](ClO_4)_2$	*a*
3	$[\{Mn(bpy)(H_2O)\}_2(\mu\text{-}ClCH_2COO)_2(\mu\text{-}O)](NO_3)_2$	*a*
4	$[\{Mn(bpy)(H_2O)\}_2(\mu\text{-}CH_3COO)_2(\mu\text{-}O)](NO_3)_2$	*a*
9	$[\{Mn(bpy)(H_2O)\}_2(\mu\text{-}CH_3COO)_2(\mu\text{-}O)](PF_6)_2$	12
10	$[\{Mn(OH)(bpy)\}(\mu\text{-}PhCOO)_2(\mu\text{-}O)\{Mn(NO_3)(bpy)\}]$	13
	Mononuclear Mn(II) Compounds	
5	$[Mn(NO_3)_2(bpy)_2][Mn(NO_3)(bpy)_2(H_2O)]NO_3$	*a*
6	$[Mn(bpy)_3](ClO_4)_2$	*a*
7	$[Mn(phen)_3](ClO_4)_2$	*a*
8	$[Mn(bpy)_3](ClO_4)_2 \cdot 0.5C_6H_4-1,2\text{-}(COOEt)_2 \cdot 0.5H_2O$	*a*

[a] This paper.

analogous to **4** has been described in the literature, $[\{Mn(bpy)(H_2O)\}_2(\mu\text{-}CH_3COO)_2(\mu\text{-}O)](PF_6)_2$ (**9**).[12] The cationic complex is the same, and only the counteranion is different (nitrate for compound **4**). On the other hand, as has been pointed out previously, the nitrate anion shows a certain tendency to act as a ligand. A binuclear Mn(III) complex with nitrate ligand $[\{Mn(OH)(bpy)\}(\mu\text{-}PhCOO)_2(\mu\text{-}O)\{Mn(NO_3)(bpy)\}] \cdot H_2O$ (**10**) has been reported in the literature.[13] Thus, the coordination of the nitrate anion cannot be excluded a priori for compound **4**. So, we also recorded the XANES and EXAFS spectra of these two compounds described in the literature and previously synthesized **9**[12] and **10**.[13]

The normalized XANES spectra at the Mn K-edge for compounds **1**−**4**, **9**, and **10** (Figure 5A), are almost superimposable, as we could expect, because all of them show the same sort of binuclear Mn(III) complex: $[\{Mn(nn)L\}_2(\mu\text{-}RCOO)_2(\mu\text{-}O)]^{2+}$ (nn = bpy, except for **2** where nn = phen, L = H_2O, except for **10** where L = NO_3 and OH. R = $ClCH_2$ for **1**, **2**, and **3**, CH_3 for **4** and **9**, and Ph for **10**). Nevertheless, their corresponding second derivatives (Figure 5B) show small differences due to the differences in the crystallographic structures. Several distinct near-edge features are indicated on the plot of the XANES spectra. *P* is a pre-edge peak arising from a dipole forbidden, but quadrupole allowed, 1s → 3d inner atomic transition in an octahedral

(41) Gelasco, A.; Askenas, A.; Pecoraro, V. L. *Inorg. Chem.* **1996**, *35*, 1419.

Table 6. XANES Analysis Results for Compounds **1**−**4**, **9**, and **10** and Distance Information from Crystal Structure Data and/or EXAFS Fitting

					RMS deviation[d]		
	P'[a]	P''[a]	E[b]	M[c]	RX	EXAFS	1s → 3d area[e]
1	6538.7	6541.3	6549.3	6557.5	0.15	0.15	12.35
2	6538.7	6541.3	6549.4	6557.8		0.15	12.82
3	6538.5	6541.3	6549.3	6557.5	0.15	0.15	11.96
4	6538.5	6541.3	6549.4	6557.7		0.15	13.04
9	6538.7	6541.4	6549.6	6557.7	0.17	0.16	13.26
10	6538.8	6541.7	6549.6	6557.1	0.14	0.14	11.27

[a] Pre-edge energies (P' and P''), eV. [b] Edge energy (E) refers to the energy at the first inflection point of the normalized edge (IPE), eV. [c] Energy of the edge maximum (M), eV. [d] Root-mean-square deviation in Mn first coordination N_2O_4 sphere distances, Å. [e] Area for the 1s → 3d region, eV × 10^{-2}.

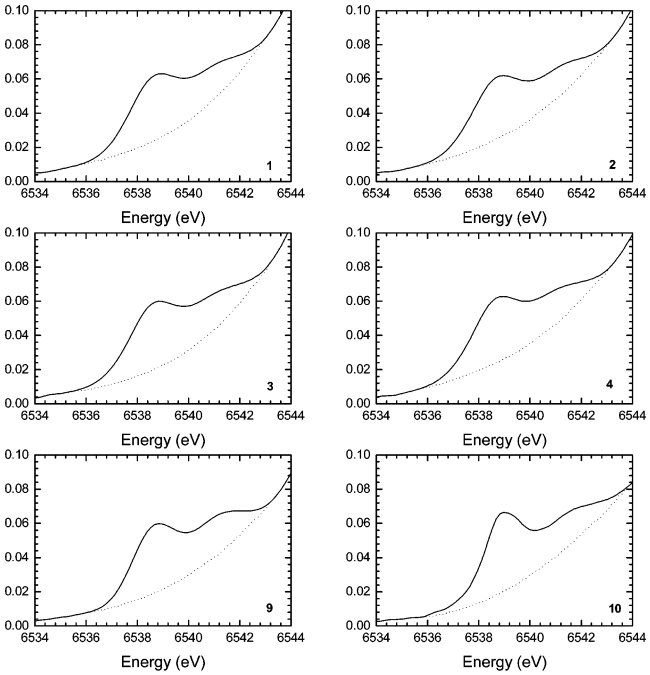

Figure 6. 1s → 3d region of the XANES spectra (—) with background polynomial (- - -) for compounds **1**−**4**, **9**, and **10**.

MnO_6 environment. The observed doublet in the pre-edge feature (P' and P'') is due to a crystal-field splitting of Mn 3d states into t_{2g} and e_g orbitals. E is associated with Mn 1s transitions into p-like states of t_{1u} symmetry, and M is the main peak ("white line") of the Mn K absorption spectra. The plot of second derivates is labeled accordingly. The XANES analysis results for compounds **1**−**4**, **9**, and **10** are shown in Table 6.

All XANES spectra show a noticeable pre-edge peak centered at 6539 eV (Figure 6). The magnitude of this peak depends on coordination number and symmetry, and in general, the 1s → 3d area increases with increased bond-length disorder. The measured area of the pre-edge peak in electron-volts × 10^{-2} was 12.35, 12.82, 11.96, 13.04, 13.26, and 11.27 for compounds **1**−**4**, **9**, and **10**, respectively. Compound **9**, with a major RMS deviation (0.16), shows a major area value, and **10**, with smaller RMS deviation (0.14), shows a minor area value. Compounds **1**−**4**, with the same RMS deviation (0.15), show an intermediate area value. To the best of our knowledge, this region of the XANES spectra has not been studied for other Mn(III) binuclear compounds. A comparative study of the 1s → 3d area for Mn(II) complexes and enzymes is reported in the literature.[9a] For the binuclear complex $[\{Mn(HB\text{-}3,5\text{-}^iPr_2pz)_3\}_2(\mu\text{-}OH)_2]$, where the manganese ions are five-coordinated with an RMS = 0.08, the area was 12.4 × 10^{-2},[40,9a] while for the tetranuclear complex $[Mn(2\text{-}OHpicpn)]_4(ClO_4)_4$, where the octahedron around the manganese ions is highly disordered, the RMS = 0.12 and the area was 14.3 × 10^{-2}.[41,9a] Four binuclear Mn(II) enzymes with a six-coordinate complex were reported in the literature: Mn-ribonucleotide reductase and arginase, with an area value of 7.2−7.8 × 10^{-2} eV,[9a] and catalase and Mn-hemerythrin, where the area was 10.0−12.3 × 10^{-2} eV,[9a] indicative of a highly disordered polyhedron of coordination. Finally, for the superoxidized Mn-catalase (Mn^{III}/Mn^{IV}), the area was 14.5 × 10^{-2} eV.[9b]

For Mn(III) complexes with Jahn-Teller distortion, a larger area and RMS than for Mn(II) compounds could be expected, but in the experimental results there are no important differences between the Mn(II) and Mn(III) complexes. On the other hand, the higher value reported for the superoxidized manganese catalase could be due to the presence of two different oxidation states. For compounds **2** and **4**, the area values are a bit higher than for **1** and **3**; thus, a similar or a slightly greater disorder in the distances around the manganese centers could be expected.

It has been shown that the position of the K-edge depends on (a) the oxidation state of the manganese (higher inflection point energy (IPE) was found for a higher oxidation state) and (b) the nature of the ligands (the metal atom with more electron-donating ligands is generally characterized by a lower IPE). But the magnitude of the shift is not the same in both cases. The change of the oxidation state in bi-, tri-, and tetranuclear complexes of manganese with similar coordination environment leads to shifts of 1−2 eV;[10] nevertheless, significant structural changes in complexes of equal oxidation state, such as the replacement of a di-μ-oxo bridge by a mono-μ-oxo and μ-acetato bridges, result in shifts of only 0.5−0.6 eV.[10] In this context, we would expect the compounds examined here to show very similar IPE values, as is observed: the effect of the chloride in the carboxylate bridge does not seem to be important. The only IPE reported in the literature for a Mn(III) binuclear complex is 6549.6 eV for $[\{Mn(tmtacn)\}_2(\mu\text{-}CH_3COO)_2(\mu\text{-}O)](ClO_4)_2$.[10] Taking into account the correlation of IPE data as a function of the mean N/O ratio of the Mn ligands in the complex, postulated by Kuzek and Pace,[8b] we could expect higher IPE values for the compounds described here (with a N/O ratio of 0.5) than for the complex with the tridentate amine tmtacn (with a N/O ratio of 1). Nevertheless, the IPE values found for compounds **1**−**4** are equal or even lower than the IPE reported for the compound with tmtacn. On the other hand, the IPEs of the binuclear Mn(III) compounds described here are in good agreement with those reported for different binuclear enzymes in the reduced form Mn(II)Mn(II), which are slightly lower, i.e., 6548.0 eV for Mn-hemerythrin (N/O = 0.83),[9a] 6549.0 eV for the ribonucleotide reductase (N/O = 0.33),[9a] and 6549.2 eV for the arginase (N/O = 0.25).[9a] Also, the IPE reported for the S_0 state of the OEC, 6551.7

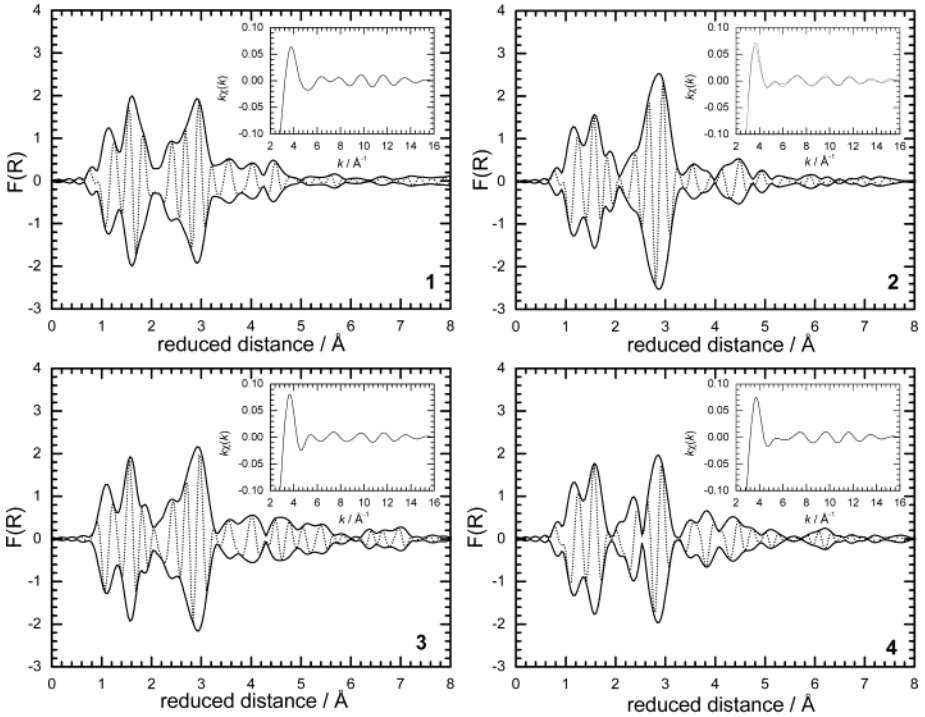

Figure 7. k^3-weighted Fourier transforms (modulus and imaginary part) of normalized EXAFS oscillations at the manganese K-edge for compounds **1**−**4**. In the inset, the *k*-weighted EXAFS oscillations corresponding to filtered signal: (- - -) experimental data; (—) simulations (parameters listed in Table 7) for compounds **1**−**4**.

eV,[5] is higher, as could be expected, due to the higher oxidation state of this site (postulated as $Mn_3^{III}Mn^{IV}$).

Figure 7 shows the Fourier transforms (FTs) of the experimental EXAFS oscillations at the manganese K-edge and in the inset (dashed lines), with the experimental filtered EXAFS signal corresponding to the first peak of the FTs for compounds **1**−**4**. The EXAFS is related to the backscattering of electrons released from the X-ray absorbing center (Mn) by ligands of the first few coordination spheres. Peaks in the Fourier transformed EXAFS spectrum correspond to "backscattering" ligands of Mn at a Mn−ligand distance, which is about 0.4 Å greater than the "reduced" distance in Figure 7. In all cases, FTs could be seen as two main peaks, where each one could comprise several shells. For compounds **1** and **3**, and depending on their crystal structures, the first peak corresponds to the first atomic shell surrounding the manganese center. In these compounds, this shell contains two nitrogen atoms from the bidentate amine (bpy or phen) and four oxygen atoms (two of them of the carboxylate bridges, one of the monodentate ligand, water, and one of the oxo bridge). The second peak (∼3 Å) corresponds to the second atomic shell (carbon of the amine and carboxylate ligands) and mainly to 2.7 Å Mn−Mn interactions.[42] The chloride of the carboxylate bridge must appear at greater distances.

The two models considered are the two compounds described in the literature: compound **9**, $[\{Mn(bpy)(H_2O)\}_2(\mu\text{-}CH_3COO)_2(\mu\text{-}O)](PF_6)_2$,[12] with two water ligands, and **10**, $[\{Mn(OH)(bpy)\}(\mu\text{-}PhCOO)_2(\mu\text{-}O)\{Mn(NO_3)(bpy)\}]\cdot H_2O$, with a coordinated anion.[13] As we expected, the experimental spectra of **1** and **3** are similar to the spectrum of compound **9** (and significantly different from the spectrum of compound **10**) (Figure S2, Supporting Information). The same result was observed when the experimental spectra of compounds **2** and **4** were compared with the spectra of **9** and **10**. From these results, we conclude that in compounds **2** and **4** (whose structures have not been characterized by X-ray diffraction) the counteranion does not form a part of the first coordination sphere of manganese, and the labile position in each manganese ion must be occupied by a water ligand, as in compounds **1**, **3**, and **9**. The results of the fit for the four compounds are shown in Table 7. Comparison of the results obtained by EXAFS and X-ray diffraction for compounds **1** and **3** shows a good agreement between both techniques. Three differentiated Mn−O distances could be found: the shorter one, corresponding to the Mn−O bridge distance, the next distance, corresponding to the Mn−O carboxylate cis to the oxo bridge (see Scheme 1), and two longer distances, with an average value of 2.22 Å for all compounds (**1**−**4**). For compounds **1** and **3**, the longer distances correspond to the ligands on the Jahn-Teller axis: the waterligand ($Mn-O_w$) and the other O-carboxylate ($Mn-O_{trans}$). Thus, for compounds **2** and **4** the longer distances could be assigned to the same ligands. Nevertheless, compounds **1** and **3** show different $Mn-O_w$ and $Mn-O_{trans}$

Scheme 1

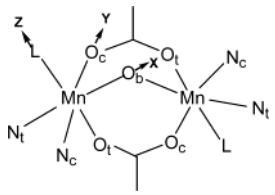

(42) Penner-Hahn, J. E. *Struct. Bonding* **1998**, *90*, 1−36.

Table 7. Mn−Nearest Neighbor EXAFS Fitting Results for **1**−**4**[a]

	Mn−O_b		Mn−O_{cis}		Mn−N		Mn−O	
	N	*R*(*σ*)	*N*	*R*(*σ*)	*N*	*R*(*σ*)	*N*	*R*(*σ*)
1	1	1.79(0.06)	1	1.95(0.07)	2	2.06(0.08)	2	2.22(0.12)
2	1	1.79(0.06)	1	1.96(0.07)	2	2.06(0.08)	2	2.22(0.09)
3	1	1.79(0.06)	1	1.96(0.06)	2	2.07(0.07)	2	2.22(0.09)
4	1	1.79(0.06)	1	1.96(0.07)	2	2.07(0.07)	2	2.22(0.10)

[a] *N* is the number of neighboring atoms at the distance *R* (in Å) from the manganese center, with the Debye−Waller factors *σ* (in Å) given in parentheses. The mean-electron-free path *λ* was chosen as $\lambda(k) = (1/\Gamma)[(\eta/k)^4 + k]$ with $\eta = 3.1$ and $\Gamma = 0.6$ eV, values that were obtained from model compound **9**. *N* in each shell is fixed whereas *σ* and *R* were fitted. The ΔE_0 parameter was also allowed to vary but using a single value because of similar absorber−scatterer pairs[45] (−6.0, −5.7, −5.8, and −5.1 eV for **1**−**4**, respectively). The residual factor defined as $\sum(k\chi_{exp} - k\chi_{th})^2/\sum k\chi_{exp}^2$ was 0.026, 0.026, 0.022, and 0.014 for compounds **1**−**4**, respectively. In the Supporting Information, the details of the results of the 4 adjustments are given.

Table 8. Mn(II) Compounds Obtained after the Reaction of the Binuclear Mn(III) Complexes $[\{Mn(nn)(H_2O)\}_2(\mu\text{-}RCOO)_2(\mu\text{-}O)](X)_2$ with H_2O_2 in Absence or in Presence of an Excess of $NaClO_4$

compd	H_2O_2	$H_2O_2 + NaClO_4$
1	$[Mn_3(bpy)_2(\mu\text{-}ClCH_2COO)_6]$[39]	
2	$[\{Mn(phen)_2\}_2(\mu\text{-}ClCH_2COO)_2](ClO_4)_2$[39]	
3	$[Mn_3(bpy)_2(\mu\text{-}ClCH_2COO)_6]$ [39]	$[Mn(bpy)_3](ClO_4)_2$ (**6**)
4	$[Mn(NO_3)_2(bpy)_2][Mn(NO_3)(bpy)_2(H_2O)]\ NO_3$ (**5**)	$[Mn(bpy)_3](ClO_4)_2$ (**6**)

distances, and also, the distortion around each manganese ion is a bit different. Unfortunately, these variations are not sufficient to be distinguished by EXAFS spectroscopy.

Reactivity in Front of H_2O_2. The reactions of the brown solutions of the binuclear Mn(III) complexes $[\{Mn(nn)(H_2O)\}_2(\mu\text{-}RCOO)_2(\mu\text{-}O)]X_2$ (**1**−**4**) with a large excess of H_2O_2 (more than 500 times the stoichiometric proportion) were exothermic. The color of the solutions turned immediately to yellow, and a great evolution of oxygen was observed, in all cases. After this first step, in which the $Mn^{III}-Mn^{III}$ complex was reduced, the system entered a catalytic cycle, with alternating coloration and discoloration of the solution, and monotonic evolution of oxygen. After 15 min, a little brown residue could be observed, along with a perceptible reduction in the emission of oxygen. After 1 h, the evolution of oxygen had nearly stopped.

When the evolution of oxygen stopped, the small amount of brown residue was filtered. Unfortunately, there was not enough of this residue to characterize it, but IR spectra showed a broad band, characteristic of manganese oxides. The formation of this product was probably due to the decomposition of the catalytic species. The final solutions were left undisturbed, and Mn(II) complexes with different nuclearity were obtained. For the starting Mn(III) binuclear complexes with nitrate anion (**1** and **3**), addition of an excess of $NaClO_4$ to the final solution was also tested, with the aim to see the effect of the anion in the final Mn(II) compound (Table 8).

Compounds **1** and **3**, with the same cationic entity $[\{Mn(bpy)(H_2O)\}_2(\mu\text{-}ClCH_2COO)_2(\mu\text{-}O)]^{2+}$ and different counteranion (ClO_4^- or NO_3^-) gave the trinuclear complex described in the literature $[Mn_3(bpy)_2(\mu\text{-}ClCH_2COO)_6]$.[39] On the other hand, compound **2**, $[\{Mn(phen)(H_2O)\}_2(\mu\text{-}ClCH_2COO)_2(\mu\text{-}O)](ClO_4)_2$, gave the binuclear complex $[\{Mn(phen)_2\}_2(\mu\text{-}ClCH_2COO)_2](ClO_4)_2$.[39] Nevertheless, the reaction of compound **3** with H_2O_2 and an excess of $NaClO_4$ gave only the mononuclear compound without carboxylate, $[Mn(bpy)_3](ClO_4)_2$ (**6**). In the same way, in the reactions with the acetate complex $[\{Mn(bpy)(H_2O)\}_2(\mu\text{-}CH_3COO)_2(\mu\text{-}O)](NO_3)_2$ (**4**), only mononuclear complexes without carboxylate, **5** or **6** (when $NaClO_4$ was added), were obtained.

In a previous work,[39] we tried to synthesize the binuclear and trinuclear Mn(II) complexes with $ClCH_2COO^-$ and CH_3COO^-, but the binuclear complex with bpy ligand, $[\{Mn(bpy)_2\}_2(\mu\text{-}ClCH_2COO)_2](ClO_4)_2$, was not obtained. This is in agreement with the results obtained here for the reduction of compounds **1** and **3** by H_2O_2, where the neutral trinuclear complex is formed when nitrate or a small amount of perchlorate anion is present. A significant excess of perchlorate anion provokes the formation of an ionic complex: in this case, the most stable species was the mononuclear complex without carboxylate ligand.

Syntheses of Mn(II) complexes with phenanthroline ligand[39] gave two compounds: an ionic binuclear Mn(II) complex and a neutral chain. By reduction of Mn(III) binuclear complex **2**, where the perchlorate anion was present, the ionic species was formed.

The most surprising result was found with the acetate complex, **4**. Both Mn(II) compounds are described in the literature, the ionic binuclear complex $[\{Mn(bpy)_2\}_2(\mu\text{-}CH_3COO)_2](ClO_4)_2$[46] and the neutral trinuclear $[Mn_3(bpy)_2(\mu\text{-}CH_3COO)_6]$,[47] but none of them was found by reduction of the binuclear Mn(III) complex. Only mononuclear compounds without carboxylate ligand were obtained. Because of the higher basicity of the acetate ligand, the carboxylic group could be protonated under the reaction conditions, and the volatility of acetic acid may contribute to the decoordination of these carboxylate ligands.

Measurement of the volume of evolved O_2 showed, after 2 h, a decomposition of ∼70% of H_2O_2 equivalent to 230 turnover numbers (tons) (see Scheme 2). Figure 8 shows the catalytic disproportionation of the H_2O_2 with the binuclear Mn(III) complexes (**1**−**4**). Significant differences between the nitrate compounds (**3** and **4**) and perchlorate compounds (**1** and **2**) could be observed. With the nitrate complexes, more than 70% of the initial H_2O_2 decomposed after 1 h of reaction (280 tons for **3** and 250 tons for **4**), while with the perchlorate compounds, less than 60% of H_2O_2 decomposed (185 tons for **1** and 160 tons for **2**). If we compare the results obtained for compounds **1** and **3** with the same cationic complex, there is a major extension of the reaction and a faster H_2O_2 decomposition for the nitrate complex than for the perchlorate complex.

(43) Hong, D. M.; Chu, Y. Y.; Wei, H. H. *Polyhedron* **1996**, *15*, 447.
(44) McCann, M.; Casey, M. T.; Devereux, M.; Curran, M.; Cardin, C.; Todd, A. *Polyhedron* **1996**, *15*, 2117.
(45) Michalowicz, A.; Vlaic, G. *J. Synchrotron Radiat.* **1998**, *5*, 1317.
(46) Rardin, R. L.; Tolman, W. B.; Lippard, S. J. *New J. Chem.* **1991**, *15*, 417.
(47) Ménage, S.; Vitols, S. E.; Bergerat, P.; Codjovi, E.; Kahn, O.; Girerd, J.-J.; Guillot, M.; Solans, X.; Calvet, T. *Inorg. Chem.* **1991**, *30*, 2666.

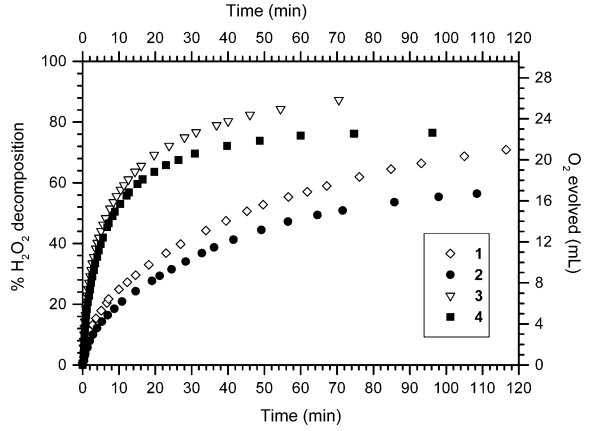

Figure 8. Catalytic disproportionation of H_2O_2 with binuclear Mn(III) complexes, in CH_3CN. $[Mn^{III}-Mn^{III}] = 0.8$ mM, $[H_2O_2] = 0.53$ M.

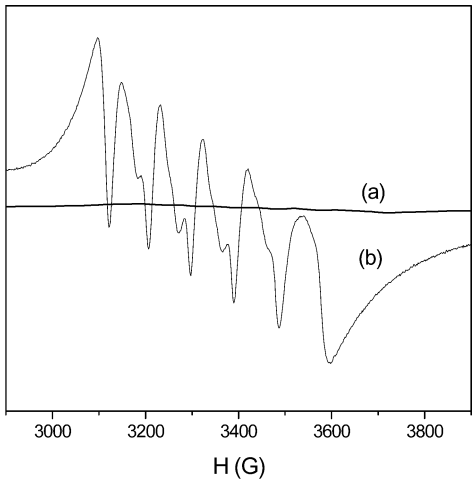

Figure 9. EPR spectra at 77 K: (a) initial solution of **1** in MeCN, (b) 1 min after the addition of H_2O_2.

Scheme 2

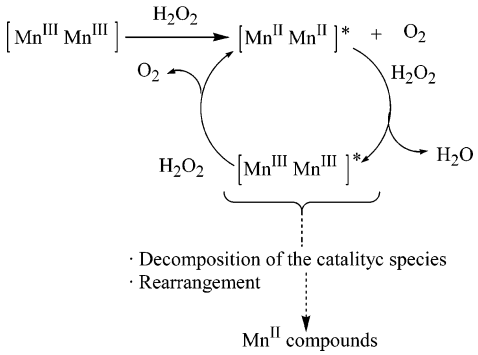

Following the reaction of the binuclear Mn(III) complexes with H_2O_2 by EPR spectroscopy, the formation of mixed-valence species could be discarded. Figure 9 shows the spectrum of the starting Mn(III) solution, and the spectrum after 1 min of reaction. The spectra after 15 min and after 1 h of reaction were superimposable. These spectra show, in the region of $g \approx 2$, six intense bands with some other superimposed bands (Figure 9). This kind of spectrum is characteristic of a Mn(II) compound with small zero field splitting. The spectra could be simulated with a hyperfine coupling of ~90 G and a ZFS value of ~50 G. No evidence of a $Mn^{II}-Mn^{III}$ or $Mn^{III}-Mn^{IV}$ system was observed in any case. This may agree with a catalytic cycle that runs between $Mn^{II}-Mn^{II}$ and $Mn^{III}-Mn^{III}$.

Binuclear Mn(II) complexes with important magnetic exchange show usually different spectra, with more bands.[48] In a previous work,[39] we reported the magnetic properties of polynuclear Mn(II) complexes with chloroacetate bridges. When only two carboxylate bridges are present, the magnetic coupling is very small, and the EPR spectra in solution also showed the characteristic pattern of an isolated Mn(II) ion. Nevertheless, the stability of these compounds in solution was confirmed by electrospray mass spectrometry.[49] Then, if the Mn(II) catalytic species is a binuclear complex with carboxylate ligands, it could be seen in EPR spectroscopy as an isolated Mn(II) ion, and it is not possible to be confident about the existence of the binuclear catalytic complex.

Conductivity measurements were carried out for the initial solution of compounds **1** and **3**, and, after the addition of the H_2O_2, for a period of 2 h; the molar conductivity remains constant (~290 Ω^{-1} cm^2 mol^{-1}). If the binuclear complex was broken in mononuclear fragments, the conductivity would be higher, while along the reaction the conductivity values correspond to a 2:1 electrolyte. Two days later, after the decomposition of the catalytic species, the molar conductivity increased considerably (×30) probably because of the fragmentation of the binuclear complexes.

The ES-MS spectrum of the solution of compound **1** at 1 min of the beginning of the reaction showed two peaks corresponding to binuclear species of Mn(II), $[Mn_2(bpy)_2(ClCH_2COO)_3]^+$ (m/z = 701.2) and $[Mn_2(bpy)_2(ClCH_2COO)_2(H_2O)(OH)]^+$ (m/z = 643.1), and several peaks corresponding to different mononuclear fragments. Unfortunately, it was not possible to see any peak of the Mn(III) fragments. We have observed that for the binuclear Mn(III) complexes the concentration of the solution has to be higher to detect the molecular peak and the fragments. That is, in the experimental conditions of the reaction, the Mn(III) concentration may not be enough to detect the Mn(III) catalytic species by this technique.

The results obtained by these techniques seem to agree with the preservation of the binuclear structure during the reaction. With the aim to see if the formation of $[Mn_2(bpy)_2(ClCH_2COO)_3]^+$ was necessary for the catalytic activity, the reaction was tested again, adding more $ClCH_2COOH$, in a 1:1 proportion, to the solution of the Mn(III) binuclear complex $[\{Mn(bpy)(H_2O)\}_2(\mu\text{-}ClCH_2COO)_2(\mu\text{-}O)](ClO_4)_2$. The reduction of the Mn(III) complex was very fast, and the evolution of O_2 stopped immediately; measurement of the evolved O_2 showed a decomposition of ~6% of H_2O_2 (20 tons). This fact discarded the hypothesis of the formation of $[Mn_2(bpy)_2(ClCH_2COO)_3]^+$ as intermediate catalytic species. After these results, a system with $[\{Mn(bpy)\}_2(\mu\text{-}ClCH_2COO)_2]^{2+}$ core could be postulated. Then, the reaction

(48) (a) Laskowski, E. J.; Hendrickson, D. W. *Inorg. Chem.* **1978**, *17*, 457. (b) Blanchard, S.; Blondin, G.; Riviere, E.; Nierlich, M.; Girerd, J. J. *Inorg. Chem.* **2003**, *42*, 4568.

(49) Λ_M in MeCN, 10^{-3} M = 223 Ω^{-1} cm^2 mol^{-1}; the expected Λ_M values in this solvent for 1:2 electrolytes are in the range 220−300 Ω^{-1} cm^2 mol^{-1}. ESP(+): CH_3CN/CH_3OH, m/z =508.8 corresponding to $[\{Mn(phen)_2\}(\mu\text{-}ClCH_2COO)_2]^{2+}$.

Scheme 3

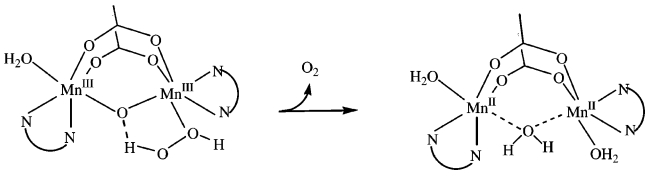

between the binuclear Mn(III) complexes with H_2O_2 could be summarized in three steps: reduction, catalytic cycle, and finally decomposition of the catalyst and crystallization of Mn(II) compounds (Scheme 2).

The starting binuclear Mn(III) complexes show two labile positions, one in each manganese ion, occupied by water ligands. In a first step, a water ligand could be replaced by H_2O_2, and monodentate coordination could be stabilized by hydrogen bonding with the oxo ligand and/or with the carboxylate bridges. This interaction could favor the reduction of both manganese ions and the evolution of O_2. Using a mechanism similar to the one postulated for the catalase,[2,4] the oxo bridge could be protonated, hence becoming a water or a hydroxo ligand (Scheme 3).

The catalytic Mn(II) binuclear complex $[Mn^{II}-Mn^{II}]^*$ would have two labile positions in each manganese ion: this intermediate could be very sensitive to rearrangements, and this is probably the reason for the decomposition of the catalyst.

When the binuclear Mn(II) compound $[\{Mn(phen)_2\}_2(\mu\text{-}ClCH_2COO)_2](ClO_4)_2$ was treated with H_2O_2, no reaction was observed. In this complex, the Mn(II) ions show two bidentate amines and two carboxylate bridges, so no labile position to coordinate the H_2O_2 is present. This fact supports the idea that the carboxylate was not decoordinated and that the catalytic system needs a more labile ligand.

If the Mn(III)−Mn(III) catalytic species must regenerate the oxo bridge, the easiest way to do it could be the mechanism proposed for the catalase of the *Lactobacillus plantarum*, in which the H_2O_2 molecule interacts with both Mn(II) ions in a $\mu_{1,1}$ fashion.[2,4] In our case, this intermediate could be stabilized by hydrogen bonds with terminal water ligands.

Magnetic Properties. For compound **3**, the magnetization study at 2 K was carried out. The molar magnetization is linear in magnetic field only until 9000 G, so the magnetic measurements were recorded at 8000 G for all compounds. The magnetic susceptibility of **1**−**4** was measured in the range 4−300 K (Figure 10). In all cases, the $\chi_M \cdot T$ product decreases with the temperature. This behavior is characteristic of an antiferromagnetic coupling between the Mn(III) centers. Compound **2** shows, comparatively, a greater variation of $\chi_M \cdot T$ with the temperature than the others. For this compound, a maximum on the χ_M versus T plot was observed at 29.6 K. For the other compounds, this maximum appears at lower temperatures (compound **1**, at 9.5 K; compound **4**, at 7.7 K; and for compound **3**, it was not observed).

For antiferromagnetic systems, magnetic susceptibility is not highly sensitive to the zero-field splitting of Mn(III) ions. Then, a simple Heisenberg Hamiltonian $H = -JS_1 \cdot S_2$ could be used to fit the experimental data. Assuming that the two

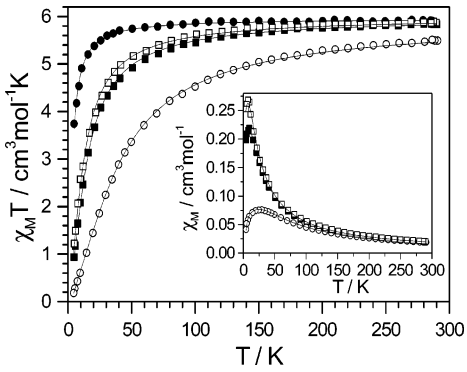

Figure 10. $\chi_M \cdot T$ vs T plot for **1** (■), **2** (○), **3** (●), and **4** (□). The inset shows χ_M vs T plot for **1**, **2**, and **4**; the solid line is the best fit to the experimental data.

Mn(III) ions have the same isotropic g value, from the Van Vleck formula, the $\chi_M \cdot T$ expression for two $S = 2$ ions is given in eq 1

$$\chi_M \cdot T = \frac{2Ng^2\beta^2}{k} \frac{30\exp(10x) + 14\exp(6x) + 5\exp(3x) + \exp(x)}{9\exp(10x) + 7\exp(6x) + 5\exp(3x) + 3\exp(x) + 1} \quad (1)$$

where $x = J/kT$.

The best fits were obtained with $J = -2.89$ cm^{-1} and $g = 1.99$, with $R = 8.1 \times 10^{-6}$ (compound **1**), $J = -8.16$ cm^{-1} and $g = 1.99$, with $R = 3.1 \times 10^{-4}$ (compound **2**), $J = -0.68$ cm^{-1} and $g = 1.99$, with $R = 2.8 \times 10^{-5}$ (compound **3**), and $J = -2.34$ cm^{-1} and $g = 1.98$, with $R = 3.8 \times 10^{-4}$ (compound **4**) (Figure 10).

For these compounds, in particular for compound **3**, with little antiferromagnetic interaction, it is necessary to verify if the shape of the $\chi_M \cdot T$ versus T plot was due to the magnetic exchange or to the zero-field splitting of the Mn(III) ions. So, we also fitted the data taking into account both factors (the zero-field splitting and the intradimer exchange coupling), by using the spin Hamiltonian $H = -JS_1 \cdot S_2 + S_1 \cdot D_1 \cdot S_1 + S_2 \cdot D_2 \cdot S_2 + (g_1S_1 + g_2S_2)\beta H$. A program supplied by D. Gatteschi[50] was used to find the energy levels as functions of the magnetic field. Assuming $D_1 = D_2$ and $g_1 = g_2$, we found that for **1** and **4** the D value is practically zero (2.2×10^{-6} and 4.3×10^{-6} cm^{-1}, respectively), and $J = -2.96$ cm^{-1}, $g = 2.0$ for **1** ($R = 3.5 \times 10^{-5}$), and $J = -2.45$ cm^{-1}, $g = 2.0$ for **4** (7.4×10^{-5}). For compound **2**, the best fit corresponded to $J = -8.32$ cm^{-1}, $g = 2.0$, and $D = -0.81$ cm^{-1} (1.6×10^{-5}), while for **3** we found $J = -0.67$ cm^{-1}, $g = 2.0$, and $D = -0.11$ cm^{-1} (2.6×10^{-5}). In all cases, the J and g values obtained are very similar to those found without considering the zero field splitting parameter D (eq 1). Moreover, the experimental $\chi_M \cdot T$ value for compound **3** could not be fitted considering only the ZFS effect ($J = 0$).

The magnitude of the magnetic exchange interactions between the two Mn(III) ions found in compounds **1**−**4** may be compared with those reported for the other binuclear Mn(III) complexes with $[Mn_2(\mu\text{-}RCOO)_2(\mu\text{-}O)]^{2+}$ core. To our

(50) Program supplied by D. Gatteschi (Firenze, Italy) and V. Tangoulis (Patras, Greece).

Table 9. Exchange Interactions[a] and Selected Structural Parameters for $[Mn_2(\mu\text{-}O)(\mu\text{-}RCOO)_2]^{2+}$ Complexes with Blocking Ligands: Tridentate Amine (nnn) or Bidentate Amine (nn) and Monodentate Ligand L[b]

	L	Mn···Mn, Å	Mn−O_b, Å	Mn−O−Mn α, deg	O_b···N_t, Å	O_c···N_c, Å	O_t···L, Å	LMnMnL τ, deg	*J* (D), cm^{-1}
				nn + L					
1 bpy	H_2O	3.17	1.79	124.7	3.85	4.01	4.44	96.9	−2.9
3 bpy	H_2O	3.17	1.79	124.6	3.86	4.02	4.44	109.7	−0.7
9 bpy	H_2O	3.13	1.78	122.9	3.85	3.99	4.47	98.4	−6.8
10 bpy	OH NO_3	3.14	1.78	124.1	3.85	4.05	4.37	94.8	+2 (4.5)
11 bpy	Cl	3.15	1.78	124.3	3.87	4.01	4.77	81.6	−8.2
12 bpy	N_3	3.15	1.80	122.0	3.89	4.19	4.25	108.2	+17.6 (0.3)
				nnn					
13 Metacn	N−	3.15	1.81	121.0	3.94	4.28	4.28	93	+18 (3)
14 tp-tacn	N−	3.16	1.80	122.3	3.93	4.20	4.27	77.3	+9.2 (2.3)
15 TMIP	N−	3.16	1.79	124.4	3.86	4.05	4.38	81.0	∼ −0.4
16 HpzB	N−	3.18	1.79	125.0	3.84	4.11	4.37	82.6	∼ −1

[a] Values using the $-JS_1 \cdot S_2$ convention. Additional details for compounds follow: **1** $[\{Mn(bpy)(H_2O)\}_2(\mu\text{-}ClCH_2COO)_2(\mu\text{-}O)](ClO_4)_2$ (this work); **3** $[\{Mn(bpy)(H_2O)\}_2(\mu\text{-}ClCH_2COO)_2(\mu\text{-}O)](NO_3)_2$ (this work). The structural parameters are the average of the parameters in both manganese centers. Trans ligand distances, for example, $O_b \cdots N_t$, are the addition of both manganese−ligand distances, $d(O_b \cdots N_t) = d(Mn-O_b) + d(Mn-N_t)$. **9** $[\{Mn(bpy)(H_2O)\}_2(\mu\text{-}CH_3COO)_2(\mu\text{-}O)](PF_6)_2$;[12] **10** $[\{Mn(OH)(bpy)\}(\mu\text{-}PhCOO)_2(\mu\text{-}O)\{Mn(NO_3)(bpy)\}]$;[13] **11** $[\{Mn(Cl)(bpy)\}_2(\mu\text{-}CH_3COO)_2(\mu\text{-}O)]$;[17] **12** $[\{Mn(N_3)(bpy)\}_2(\mu\text{-}PhCOO)_2(\mu\text{-}O)]$;[17] **13** $[\{Mn(Me_3tacn)\}_2(\mu\text{-}MeCOO)_2(\mu\text{-}O)](ClO_4)_2$;[14] **14** $[\{Mn(tp\text{-}tacn)\}_2(\mu\text{-}MeCOO)_2(\mu\text{-}O)](PF_6)_2$;[15] **15** (average of two binuclears presents in the crystal) $[\{Mn(TMIP)\}_2(\mu\text{-}MeCOO)_2(\mu\text{-}O)](ClO_4)_2$[19] and **16** $[\{Mn(HB(pz)_3)\}_2(\mu\text{-}MeCOO)_2(\mu\text{-}O)]$.[18] [b] See Scheme 1 for the terminology O_c, O_b, N_t, and N_c.

knowledge, only 8 compounds with this core are being structurally and magnetically studied.[12−19] Table 9 summarizes the most important structural parameters and the magnetic exchange interaction. Four of these compounds have a tridentate amine as blocking ligand, while the other four have a bidentate amine, and the sixth position of the octahedron is occupied by a monodentate ligand, L. The magnetic interaction can be ferro- or antiferromagnetic, with the *J* values between +18 to −8 cm^{-1}.

Several magneto-structural studies were reported in the literature for this kind of compounds. The weakness of magnetic coupling, in comparison with the analogous compounds with Fe(III), has been explained by the vacancy in the orbital z^2, pointing to the oxo-bridge ligand, for the d^4 ions.[51] The most important way for an antiferromagnetic interaction, z^2-z^2 (present in a d^5 ion), vanishes. On the other hand, the authors report the importance of the crossed interactions. The interactions involving a single occupied orbital (*xz*) and an empty orbital (z^2) are ferromagnetic. These interactions compete with the antiferromagnetic *yz*−*yz* interaction. This explains the presence of compounds with weak ferro- or antiferromagnetic interactions.

Comparison of the magnetic properties as a function of the monodentate ligand (L) for compounds **9** (L = H_2O), **11** (L = Cl), and **12** (L = N_3) in Table 9 was also reported in the literature.[17] The authors also consider the *z*-axis in the oxo-bridge direction, and antiferromagnetic coupling for **9** and **11** (H_2O and Cl) or ferromagnetic coupling for **12** (N_3) have been explained in terms of the function of the exogenous ligand and its effect in the $x^2 - y^2$ orbital. For the azido ligand, this orbital was higher in energy, and its contribution through a pathway involving the carboxylates is smaller than that for the weaker chloro and aqua ligands.

To explain the magnetic properties of compound **10** (see Table 9), new considerations were taken into account.[13] Because of the Jahn−Teller effect, the octahedron around the manganese ions could be elongated or compressed. For the compressed octahedron, the empty orbital is the z^2, pointing to the oxo-bridge ligand, while when the octahedron is elongated, the empty orbital is the $x^2 - y^2$ and the *z* axis points to the monodentate ligand L. Compounds with a compressed octahedron show ferromagnetic coupling, and an elongated environment of the manganese favors antiferromagnetic coupling. When the distortion is rhombic, a weak magnetic coupling (ferro- or antiferromagnetic) could be expected.[13]

Looking at the structural parameters, the Mn···Mn and Mn−O_b distances lie only in the ranges of 0.05 and 0.03 Å, respectively. The Mn−O_b−Mn angle is found between 121° and 125°. Considering the *x*-axis in the oxo-bridge direction and the *z*-axis in the L direction (Scheme 1), we can find the length of the octahedron axes by addition of Mn−ligand distances: $d(Mn-O_b) + d(Mn-N_t)$ (*x*-axis), $d(Mn-O_c) + d(Mn-N_c)$ (*y*-axis), and $d(Mn-L) + d(Mn-O_t)$ (*z*-axis). For all compounds, the minor distance value was found for the *x*-axis (3.84−3.94 Å), while the longer corresponded to the *z*-axis (4.25−4.77 Å). The distance for the *y*-axis was intermediate (3.99−4.28 Å). If this distance is in the superior range, similar to the distance in the *z*-direction, the octahedron is compressed in the oxo-bridge direction (*x*-axis). On the other hand, when the distance in the *y*-direction is in the low range, closer to the distance in the *x*-direction, the octahedron is elongated in the L ligand direction (*z*-axis).

Tridentate amines Me-tacn and tp-tacn favor a compressed octahedron, and a significant ferromagnetic interaction was reported for these compounds (**13**[14] and **14**[15]). Considerable compression was also observed in compound **12**, with bidentate amine and N_3 as monodentate ligand, and significant ferromagnetic coupling was also found.[17] On the other hand, with bidentate amine and monodentate ligand H_2O or Cl (**9**[12] and **11**[17]), antiferromagnetic coupling could be explained by the elongation of the octahedron.

(51) Hotzelmann, R.; Wieghardt, K.; Flörke, U.; Haupt, H.-J.; Weatherburn, D. C.; Bonvoisin, J.; Blondin, G.; Girerd, J.-J., *J. Am. Chem. Soc.* **1992**, *114*, 1681.

For compounds with tridentate amine TMIP or HpzB (**15**[19] and **16**[18]), a very weak antiferromagnetic coupling was found, and the environment of the manganese ion was rhombic in both cases (the distances in the three directions are different). A similar situation was found for compound **10**, with bidentate amine and monodentate ligand OH and NO_3.[13] In this case, the compound showed little ferromagnetic coupling.

The four compounds reported here (**1**−**4**) show an antiferromagnetic coupling that is very weak for compound **3**. Compounds **1** and **3** also present an elongated octahedral environment for the Mn(III) ions. These compounds have the same cation complex and a different counteranion, and the magnetic properties are a bit different. The same fact was observed for compounds **4** and **9**.[12] Unfortunately, it was not possible to obtain good crystals for X-ray diffraction of compound **4**.

An analogous compound of $[\{Mn(Me_3tacn)\}_2(\mu\text{-}MeCOO)_2(\mu\text{-}O)](ClO_4)_2$ (**13**)[19] with BPh_4 as counteranion was also reported,[14] but in this case, the magnetic properties are not modified by changing the anion. Compound **15**, $[\{Mn(TMIP)\}_2(\mu\text{-}MeCOO)_2(\mu\text{-}O)](ClO_4)_2$,[19] was also reported with PF_6 as counteranion, and the magnetic properties are also similar. Nevertheless, the structural characterization of these other compounds was not reported in any case.

A compound analogous to $[\{Mn(bpy)(H_2O)\}_2(\mu\text{-}CH_3COO)_2(\mu\text{-}O)](PF_6)_2$ (**9**)[12] was described in the literature with ClO_4 as counteranion.[17] In this case, the crystal structure was reported but not the magnetic measurement. The structural parameters for this compound are $d(Mn\cdots Mn) = 3.15$ Å; $d(Mn-O_b) = 1.80$ Å; $\alpha(MnOMn) = 122.8°$; $d(O_b\cdots N_t) = 3.87$ Å; $d(O_c\cdots N_c) = 4.00$ Å; $d(O_t\cdots L) = 4.45$ Å; $\tau(LMnMnL) = 94.5°$.

Thus, here we are reporting on the first cation complex $[\{Mn(bpy)(H_2O)\}_2(\mu\text{-}ClCH_2COO)_2(\mu\text{-}O)]^{2+}$ (present in compounds **1** and **3**) with two different anions, magnetically studied and characterized by X-ray diffraction. Magnetic measurements were collected for several samples (crushed crystals) of each compound and were found to be reproducible. Despite the similarity in the structural parameters, the degree of magnetic coupling for the two compounds is different. The most remarkable difference observed between the two compounds was the disposition of the two monodentate ligands, expressed by the torsion angle $\tau(L-Mn-Mn-L)$. Compound **1**, with the strongest magnetic coupling, presents the smallest torsion angle (τ) between the water molecules (Table 9).

Unfortunately, it was not possible to obtain good crystals for X-ray diffraction of compounds **2** and **4**. From the EXAFS study, an elongated environment for the manganese coordination polyhedra was postulated for both compounds, similar to **1** and **3**. The difference between **1** and **2** was the blocking bidentate amine (bpy or phen). Compound **2** shows significant antiferromagnetic coupling ($J = -8.16$ cm^{-1}), but the average elongation is similar to the average elongation of **1**. The presence of a more rigid bidentate amine could favor some differences in the distortion of the octahedron around the manganese ions and could also modify the relative disposition of these octahedrons. Both factors could explain the stronger antiferromagnetic coupling found for compound **2**.

From the EXAFS study of compound **4**, the coordination of the nitrate anion to the manganese center was ruled out. So, we could expect to have the same binuclear complex as in compound **9**. Nevertheless, the degree of magnetic coupling for the two compounds was clearly different. The average Mn−O distance in the elongation axis was also similar between compounds **4** and **9**. Thus, the weaker antiferromagnetic coupling observed for compound **4** could be due to some differences in the distortion of each coordination octahedron and their relative disposition.

In conclusion, in a general way, the magnetic properties of the four compounds reported in this work agree with the magneto-structural correlations: a more elongated octahedron gives rise to a more antiferromagnetic coupling.[13] Also, the presence of a monodentate ligand favors the elongation of the octahedron. However, other factors could also be important, such as the relative disposition of the elongation axis (τ angle). And, on the other hand, compounds with the same binuclear complex entity and different counteranions (**1** and **3**, or **4** and **9**) show different J values. These results reveal that the counteranion could not be innocent in relation to the magnetic properties of these compounds. It could play an indirect role, through the hydrogen bonds and some differences in the packing of the ions in the solid, which can give rise to differences in bond distances and angles in the binuclear Mn(III) complex, and in consequence can modify the degree of the magnetic interaction.

Conclusions

Obtaining good crystals for X-ray diffraction for two of the four binuclear compounds synthesized allowed us to compare this technique with X-ray absorption spectroscopy (XANES and EXAFS) and show the validity of these techniques for characterizing this kind of compound. It was possible to rule out the presence of an anion coordinated to the manganese centers and to postulate the elongation of the octahedron for **2** and **4**, and for **1** and **3**. Unfortunately, the structural differences for these compounds are not very important, and this technique is not sufficiently sensitive to explain the different magnitudes in the magnetic properties.

All the Mn(III) compounds reported here showed catalase activity, favored by the presence of one labile ligand coordinated to each manganese center. The catalytic species probably preserves the carboxylate bridge in the catalytic cycle, and since its slow decomposition provokes a structural rearrangement of the intermediate species, Mn(II) compounds with different nuclearity were obtained. The formation of binuclear, trinuclear, or mononuclear compounds of Mn(II) depends on stability and/or solubility. When the carboxylate was acetate, the greater volatility of the acetic acid helped aid the loss of this carboxylate, and only compounds without this ligand could be obtained. The presence of more carboxylic acid in the reaction media inhibits the catalase activity, probably by blocking labile positions in the manganese centers.

The magnetic measurements showed an antiferromagnetic interaction, which is very sensitive to the structural distortion of the manganese coordination polyhedron. For the same cation complex, different counteranions provoked differences in the distortion and disposition of the coordination octahe drons, which was reflected in the different degrees of the magnetic interaction.

Acknowledgment. This work was supported by the Dirección General de Investigación Científica y Técnica (Grant BQ2000/0791, BQ2003-00538, and BQ2001/292 to I.C.); G.F. received a Ph.D. Grant from the Universitat de Barcelona. We also wish to express our gratitude to Dr. F. Villain for help in the use of the EXAFS3 spectrometer and cryogen device, to Dr. N. Clos for recording the magnetic data, and to the student Noemí Puente for her contribution.

Supporting Information Available: X-ray crystallographic file, in CIF format, for **1**, **3**, **8**, and **9**. Additional figures and the output files of EXAFS fitting. This material is available free of charge via the Internet at http://pubs.acs.org.

IC0348897